Epidermal Growth Factor Receptor-PI3K Signaling Controls Cofilin Activity To Facilitate Herpes Simplex Virus 1 Entry into Neuronal Cells

Kai Zheng,[a,b] Yangfei Xiang,[a] Xiao Wang,[a,c] Qiaoli Wang,[a] Meigong Zhong,[a] Shaoxiang Wang,[a] Xiaoyan Wang,[a] Jianglin Fan,[d] Kaio Kitazato,[e] Yifei Wang[a]

Guangzhou Jinan Biomedicine Research and Development Center, National Engineering Research Center of Genetic Medicine, Jinan University, Guangzhou, People's Republic of China[a]; College of Life Science and Technology, Jinan University, Guangzhou, People's Republic of China[b]; School of Pharmaceutical Sciences, Sun Yat-sen University, Guangzhou, China[c]; Department of Molecular Pathology, Interdisciplinary Graduate School of Medicine and Engineering, University of Yamanashi, Chuo-City, Japan[d]; Division of Molecular Pharmacology of Infectious Agents, Department of Molecular Microbiology and Immunology, Graduate School of Biomedical Sciences, Nagasaki University, Nagasaki, Japan[e]

ABSTRACT **Herpes simplex virus type 1 (HSV-1) establishes latency in neurons and can cause severe disseminated infection with neurological impairment and high mortality. This neurodegeneration is thought to be tightly associated with virus-induced cytoskeleton disruption. Currently, the regulation pattern of the actin cytoskeleton and the involved molecular mechanisms during HSV-1 entry into neurons remain unclear. Here, we demonstrate that the entry of HSV-1 into neuronal cells induces biphasic remodeling of the actin cytoskeleton and an initial inactivation followed by the subsequent activation of cofilin, a member of the actin depolymerizing factor family that is critical for actin reorganization. The disruption of F-actin dynamics or the modulation of cofilin activity by mutation, knockdown, or overexpression affects HSV-1 entry efficacy and virus-mediated cell ruffle formation. Binding of the HSV-1 envelope initiates the epidermal growth factor receptor (EGFR)-phosphatidylinositide 3-kinase (PI3K) signaling pathway, which leads to virus-induced early cofilin phosphorylation and F-actin polymerization. Moreover, the extracellular signal-regulated kinase (ERK) kinase and Rho-associated, coiled-coil-containing protein kinase 1 (ROCK) are recruited as downstream mediators of the HSV-1-induced cofilin inactivation pathway. Inhibitors specific for those kinases significantly reduce the virus infectivity without affecting virus binding to the target cells. Additionally, lipid rafts are clustered to promote EGFR-associated signaling cascade transduction. We propose that HSV-1 hijacks cofilin to initiate infection. These results could promote a better understanding of the pathogenesis of HSV-1-induced neurological diseases.**

IMPORTANCE **The actin cytoskeleton is involved in many crucial cellular processes and acts as an obstacle to pathogen entry into host cells. Because HSV-1 establishes lifelong latency in neurons and because neuronal cytoskeletal disruption is thought to be the main cause of HSV-1-induced neurodegeneration, understanding the F-actin remodeling pattern by HSV-1 infection and the molecular interactions that facilitate HSV-1 entry into neurons is important. In this study, we showed that HSV-1 infection induces the rearrangement of the cytoskeleton as well as the initial inactivation and subsequent activation of cofilin. Then, we determined that activation of the EGFR-PI3K-Erk1/2 signaling pathway inactivates cofilin and promotes F-actin polymerization. We postulate that by regulating actin cytoskeleton dynamics, cofilin biphasic activation could represent the specific cellular machinery usurped by pathogen infection, and these results will greatly contribute to the understanding of HSV-1-induced early and complex changes in host cells that are closely linked to HSV-1 pathogenesis.**

Received 18 November 2013 **Accepted** 19 December 2013 **Published** 14 January 2014

Citation Zheng K, Xiang Y, Wang X, Wang Q, Zhong M, Wang S, Wang X, Fan J, Kitazato K, Wang Y. 2014. Epidermal growth factor receptor-PI3K signaling controls cofilin activity to facilitate herpes simplex virus 1 entry into neuronal cells. mBio 5(1):e00958-13. doi:10.1128/mBio.00958-13.

Invited Editor Carolyn Coyne, University of Pittsburgh School of Medicine **Editor** Glen Nemerow, The Scripps Research Institute

Address correspondence to Yifei Wang, twang-yf@163.com, or Kaio Kitazato, kkholi@nagasaki-u.ac.jp.

Viruses have evolved a variety of strategies to interact with host cells to initiate infection. They trigger their own cellular signaling pathways and depend greatly on the nature and physiological state of the host cells and on the interaction of the viruses with their receptors (1, 2). Because the actin cytoskeleton is a dynamic assembly of structures and is involved in many crucial cellular processes, it is not surprising that many viruses interact with actin and actin-regulating signaling pathways within the host cell (3, 4). Co-opting actin dynamics is fundamental to the diverse steps of herpesvirus biology, including entry, intracellular movement, and intercellular spreading (5). Herpes simplex virus 1 (HSV-1), a member of the alphaherpesvirus subfamily, is typically responsible for complications ranging from mucosal lesions to deadly brain infections (e.g., herpes simplex encephalitis [HSE]) (6). Infection by HSV-1 induces neurite damage and neuronal death, and virus-induced neuronal cytoskeletal disruption is the suggested cause of this neurodegeneration. Moreover, HSV-1 has been demonstrated to utilize host actin for the infection of neu-

rons, which are the cells in which the virus establishes latency and reactivates under specific conditions (7).

The role of actin during HSV-1 entry appears to be correlated with the entry mechanism and the type of cell infected, and distinct downstream signaling events have been observed (8–10). Cortical actin is the first obstacle encountered by the virus upon infection. Upon viral binding to the cellular receptor, different kinases such as Rho GTPase were triggered to modulate the cytoskeleton. In addition, efficient virus entry was achieved by the active remodeling of dynamic actin through the induction of membrane-associated receptor clustering (11, 12) and promotion of virus surfing, a process in which the virus benefits from the actin-driven mobility of these receptors to reach subcellular sites suitable for membrane fusion (13). For example, studies with human immunodeficiency virus (HIV) have demonstrated that binding of the HIV-1 gp120 protein to CD4 induces a signaling cascade that triggers actin reorganization and actin-dependent clustering of HIV-1 entry receptors to establish signaling platforms for fusion pore formation (14–16). Furthermore, multiple receptor-induced host signal molecules have been subverted by viruses to promote infection. However, in contrast to Kaposi's sarcoma-associated herpesvirus (17), very limited information is available on the cellular signaling pathways involved in the ability of HSV-1 to induce a favorable environment for entry via changes in the actin cytoskeleton. In particular, the mechanism by which HSV-1 regulates host cytoskeleton rearrangement and enters neuronal cells remains uncertain, particularly when considering that F-actin dynamics may contribute to the pathogenesis of neurological diseases and that viral entry into host cells is the most critical step for the production of virus-induced life-threatening complications (18).

In the present study, we examined the process by which HSV-1 enters neuronal cells. The results indicate that cofilin (CFL), a member of the actin depolymerizing factor family, which is important for actin dynamics and cell migration (19, 20), initiates virus infection. The HSV-1 entry-induced early biphasic dynamics of F-actin and cofilin regulation were responsible for mediating both the assembly and disassembly of F-actin. Specifically, epidermal growth factor receptor (EGFR)–phosphatidylinositide-3 kinase (PI3K) signals participated in the HSV-1-mediated early phosphorylation (inactivation) of cofilin, which triggered events facilitating actin-based receptor clustering and virus entry. We also demonstrated that extracellular signal-regulated kinase 1 (ERK) and ERK2 (Erk1/2) acted as a downstream effector controlling cofilin activity and cell ruffle formation. HSV-1 has thus evolved an intricate mechanism for infecting neuronal cells (see Fig. 8).

RESULTS

HSV-1 infection induces early actin rearrangement and cofilin biphasic activation. We used a human SK–N–SH neuroblastoma cell line to conduct the study because of their similarity to primary neuronal cells (21). This cell line is composed of morphologically distinct cell types consisting of the sympathoadrenal neuroblast (N) type and the substrate-adherent nonneuronal (S) type (22) and can be differentiated *in vitro* using various agents that promote coordinated morphological and biochemical changes leading to neuroectodermal phenotypes over a period of time (23). Moreover, undifferentiated SK–N–SH cells have previously been used to demonstrate the differences between keratinocytes and neuronal cells in response to HSV-1 infection (24). Undifferentiated cells have also been extensively used as a cellular model for studying neuropathological processes that might play a role in neurodegenerative disorders (e.g., Alzheimer's disease), making them a proper candidate for elucidating the response of neuronal cells to HSV-1 infection and the molecular interaction promoting HSV-1 entry (7, 25). The virus was added to cells at 4°C to synchronize infection before the cells were transferred to 37°C to initiate infection, a method that has been widely used (13, 26, 27). Previous studies reported that infection of HSV-1 induced filopodium formation in differentiated P19 neural cells (28); we also found that HSV-1 entry into neuronal SK–N–SH cells induced the protrusion of filopodia and lamellipodia or the formation of cortical actin at different times. As early as 10 min postinfection (mpi), we observed the dissolution of actin stress fibers and the appearance of filopodia and lamellipodia. However, stress fibers reappeared at 30 mpi (Fig. 1A). The changes in actin were analyzed semiquantitatively (Fig. 1B). In MRC-5 cells, viral infection also induced cell protrusions, such as lamellipodia and microspikes, an actin phenotype distinct from filopodia (see Fig. S1A in the supplemental material). HSV-1-induced actin remodeling was further confirmed by flow cytometry analysis. Rapid and transient actin polymerization could be observed as early as 5 mpi, and at 30 mpi, F-actin began to depolymerize (Fig. 1C). Furthermore, HSV-1 entry was impaired by the disruption of actin dynamics using three chemicals: latrunculin A (Lat-A), cytochalasin D (Cyto D), and jasplakinolide (Jas) (Fig. 1D to F). These results suggest that virus-induced actin cytoskeleton remodeling was essential for HSV-1 entry. HSV-1 entry kinetics was also examined by confocal microscopy (Fig. 1G). During the first 10 mpi, viruses were detected along the surface and were docked onto the HSV-1-induced cell protrusions (see Fig. S1B). The viruses then moved along the filopodia and were located at the cell membrane, mainly at 30 mpi, when membrane fusion and viral penetration occurred. At 60 mpi, the viruses had entered the cytoplasm and were mostly being transferred to the nucleus. In addition, at different times postinfection, intracellular internalized viral DNA was extracted and quantified. As shown in Fig. 1H, most of the virion cell entry occurred after 30 mpi. A plaque assay for viral penetration kinetics was also performed (Fig. 1I) and demonstrated a time lag between viral adsorption at 4°C and the initiation of viral penetration after a temperature shift to 37°C, which had been previously observed with HSV (29, 30). These results suggest a close correlation between the viral entry process and the timing of actin remodeling in which F-actin polymerization promotes viral binding and F-actin depolymerization facilitates viral penetration and intracellular trafficking.

Actin-filament dynamics in cells are known to be modulated by cofilin, and the most important physiological function of cofilin is to sever and depolymerize actin filaments, thereby promoting actin dynamics (31). Cofilin is inactivated by phosphorylation at serine 3, which prevents its association with actin, and is reactivated by dephosphorylation. The LIM kinases (LIMK) and testicular protein kinases phosphorylate cofilin, whereas the slingshot and chronophin phosphatases dephosphorylate cofilin at this site (32, 33). Given that HSV-1 entry induced both actin polymerization and depolymerization, we examined cofilin activity in cells infected with HSV-1 and found that cofilin was inactivated early and then activated at 30 mpi (Fig. 1J). This observation was in agreement with the quantification of the biphasic changes of

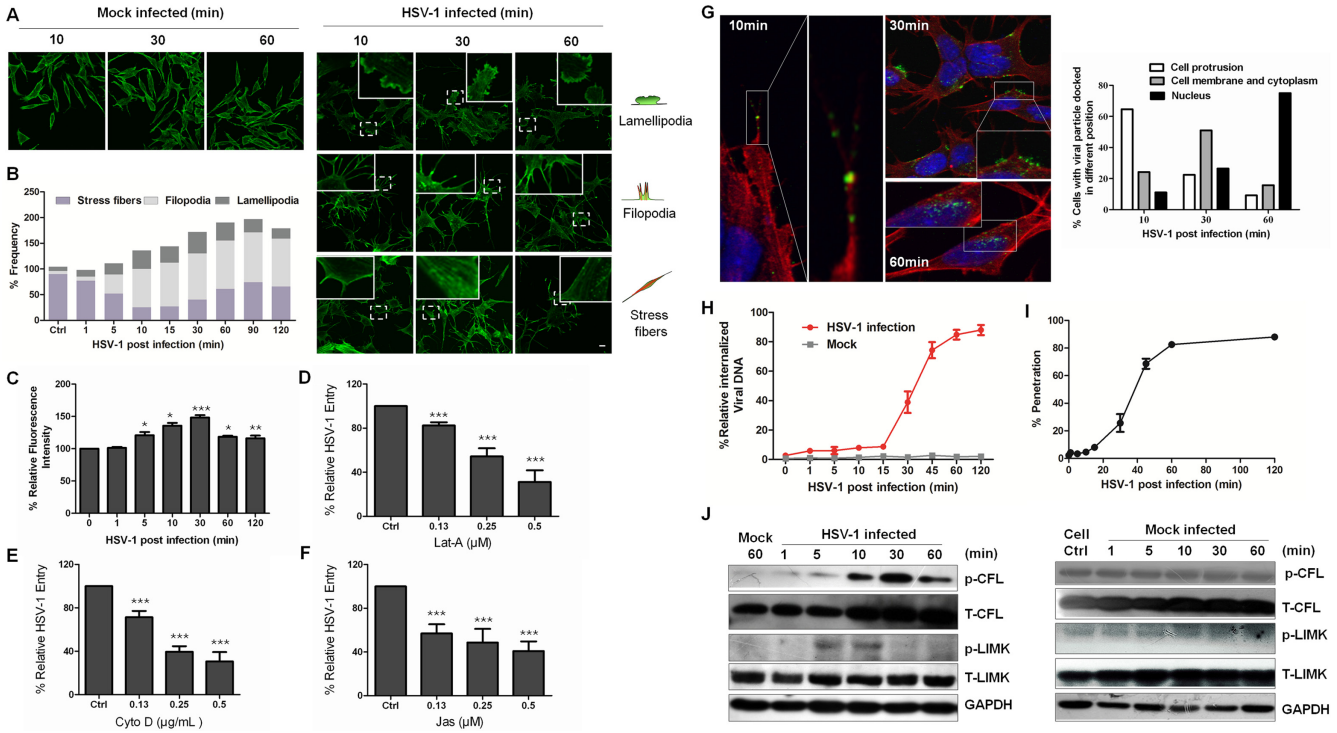

FIG 1 HSV-1 infection induces actin cytoskeleton rearrangement and biphasic activation of cofilin. (A) Formation of cell protrusions induced by HSV-1 infection. After HSV-1 (MOI 20) attachment at 4°C for 1 h, SK–N–SH cells were shifted to 37°C for the indicated times and were then stained with TRITC-phalloidin and examined by confocal microscopy. For mock infection, the cells were placed at 4°C for 1 h without virus and then moved to 37°C for the indicated times. Scale bar = 10 μm. (B) Quantification of the changes in cell ruffles at different time points postinfection. The cells with F-actin stress fibers, lamellipodia, or filopodia were designated positive cells; each value represents the mean of the results from 50 to 80 cells from at least 5 fields of 3 representative experiments. (C) Actin polymerization and depolymerization triggered by stimulation with HSV-1. F-actin was stained with FITC-phalloidin and was analyzed by flow cytometry. Each value represents the mean ± standard deviation (SD) of the results of three separate experiments. (D to F) Cytoskeleton inhibitors inhibit HSV-1 entry in a concentration-dependent manner. The cells were pretreated with Cyto D, Lat-A, or Jas at different concentrations, and HSV-1 internalization was assessed by real-time PCR (see Materials and Methods). The data are shown as the mean percent infected ± SD for three separate experiments. (G) Entry kinetics of HSV-1. Cells challenged with HSV-1 were stained with anti-ICP5 monoclonal antibody (MAb) (green), TRITC-phalloidin (red), and DAPI (blue) at the times indicated. The graph indicates the quantification of the viral particle locations at different times. At least 50 cells from five representative fields were counted in each experiment. (H) The cells bound with HSV-1 at 4°C for 1 h were transferred to 37°C; at the indicated times, bound virions that had not entered the cells were removed, and internalized viral DNA was extracted and assayed by real-time PCR. (I) Penetration assay. The cells were infected with HSV-1 at 4°C for 2 h. At various times after transfer of the cells to 37°C, virions that had not penetrated were inactivated with a pH 3 wash, and plaques were counted after 2 days. (J) Biphasic activation of cofilin and LIMK. Cofilin inactivation was measured by Western blotting using either an MAb specific for p-cofilin or an anti-cofilin pAb at the indicated time postinfection, and LIMK activation was probed using either an MAb specific for p-LIMK or an anti-LIMK MAb. In all the mock-infected experimental groups, the untreated cells were used as a control. In the HSV-1-infected group, the cells that were incubated at 4°C for 1 h and then transferred to 37°C for indicated times without HSV-1 infection to mimic infection were used as the control (mock).

F-actin (Fig. 1C). Additionally, the fluorescence intensity of phosphorylated cofilin (p-cofilin) and the colocalization of p-cofilin and F-actin demonstrated similar tendencies in the virus entry process, although most cells showed colocalization after HSV-1 infection (see Fig. S1C to F in the supplemental material). HSV-1 infection also induced a transient activation of the LIMK kinases early at 5 mpi (Fig. 1J). Taken together, these results demonstrate that the regulation of cofilin activity contributes to the HSV-1-induced dynamic remodeling of the actin cytoskeleton at early stages of infection. Viral binding (<30 mpi) requires cofilin inactivation and F-actin polymerization, whereas viral penetration and cytoplasm trafficking (30 mpi to 60 mpi) require cofilin activation and F-actin depolymerization.

Modulation of cofilin activity affects HSV-1-induced membrane ruffling and entry. To confirm the role of cofilin in HSV-1 infection, we sought to knock down or overexpress cofilin to modulate its activity because there were no direct pharmacological agents to activate or inhibit cofilin activity. During HSV-1 infection, the mRNA expression level of cofilin does not change significantly (see Fig. S2A in the supplemental material). Using small interfering RNA (siRNA), the viral entry process was clearly impeded (Fig. 2A). The cofilin (CFL)-specific siRNA inhibited 90% of cofilin expression, as detected by Western blotting, and viral entry was only 50% of the control. LIMK knockdown also inhibited HSV-1 entry (see Fig. S2B). These results suggest that cofilin is required for HSV-1 entry. The expression of mutants carrying S3E and S3A substitutions has been successfully used to mimic inactive phosphor-cofilin (p-CFL) and active cofilin, respectively. Overexpression of wild-type cofilin (WT cofilin) has also been reported to increase cofilin activity (34). To identify the role of cofilin phosphorylation in HSV-1 infection, the cells were transiently transfected with CFL/WT, CFL/S3E, and CFL/S3A. The mutant expression patterns are shown in Fig. S2C in the supplemental material. Surprisingly, the expression of both mutants of

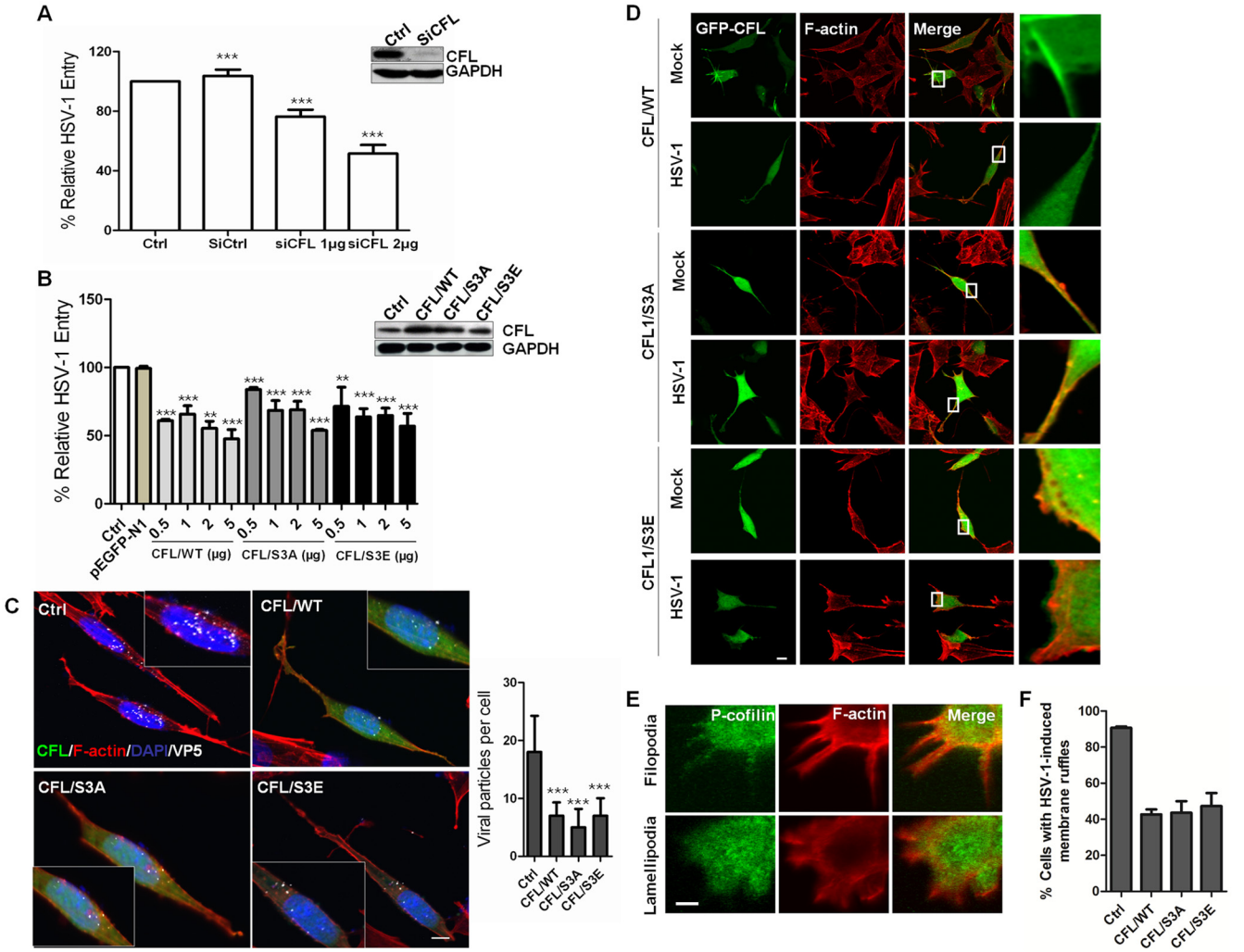

FIG 2 Role for cofilin in HSV-1-mediated membrane ruffling and entry. (A and B) HSV-1 entry is impaired by cofilin knockdown (A) or the transient overexpression of wild-type cofilin or mutants (S3A and S3E) (B). Western blot results show the knockdown or overexpression efficacy. Cells were transfected with siRNA or plasmids. At 24 h postinfection, the cells were infected with HSV-1 (MOI =20) for 1 h, and HSV-1 entry was evaluated by real-time PCR. The results are representative of three separate experiments. Ctrl, control. (C) Confocal microscopy assays showing inhibited virus entry. The cells were transfected with green fluorescent protein (GFP)-tagged plasmids (2 μg), infected with HSV-1 (MOI 20) for 1 h, fixed, and then stained with anti-ICP5 (white). Bound virions that had not entered the cells were removed by washing with cold PBS (pH 3.0). The average number of ICP5-positive capsids per nucleus was determined to evaluate viral entry. At least 50 cells with ICP5 docked at nuclei from 5 representative fields were counted in each independent experiment. (D) Active cofilin motivation during HSV-1 intracellular trafficking. The cells were infected for 60 min, stained for F-actin (red) or cofilin (green), and examined by LSM. Viral ICP5 was stained (not shown) to distinguish the infected cells from the mock-infected cells. (E) Colocalization between p-cofilin and F-actin at filopodia and lamellipodia. The cells were infected with HSV-1 and stained with either anti-p-cofilin MAb (green) or TRITC-phalloidin (red). Areas of colocalization appear yellow. (F) Overexpression of cofilin reduces the HSV-1-mediated production of cell ruffles. Cells with filopodia or lamellipodia were designated positive cells, and at least 50 cells from five representative fields were counted in each experiment.

cofilin inhibited viral entry in a dose-dependent manner, similar to the inhibition by CFL/WT (Fig. 2B). In addition, confocal microscopy detection demonstrated a reduced viral entry process. Viral particles of HSV-1 entry were visualized by immunofluorescence staining with viral protein ICP5 (Fig. 2C). At 60 mpi, more than 90% of the ICP5-positive (ICP5$^+$) particles were inside the cells, and the average number of viral particles was 18 $\pm$ 6 per cell. In contrast, the overexpression of CFL/WT, CFL/S3A, and CFL/S3E significantly reduced the total number of viral particles per cell to 7 $\pm$ 2, 5 $\pm$ 3, and 7 $\pm$ 3, respectively, but the empty vector had no effect (data not shown). Thus, the cofilin phosphocycle is critical for efficient HSV-1 entry. Both the down- and upregulation of cofilin activity inhibit viral internalization given that cofilin may accumulate progressively and transiently at cortical actin and is involved in both the assembly and disassembly of F-actin (Fig. 1C), which may affect viral binding and penetration (Fig. 1H and I). Additional microscopy experiments suggested that viral cell periphery migration mobilized the pool of active cofilin and that tight control of local active cofilin at the cell periphery is crucial for viral entry (Fig. 2D). In the absence of HSV-1 stimulation, CFL/WT-expressing cells and the overactivated mutant CFL/S3A were positive for cofilin rod-like structures. These rod-like structures consisted of active cofilin and may sequester actin monomers, thereby reducing the available G-actin sources and the

production of ruffles. These phenomena were consistent with an increased cofilin activity (32). However, HSV-1 infection changed the expression of cells expressing CFL/WT to a diffused pattern, leading to the disappearance of the rod-like structures. Viral penetration and trafficking may require active cofilin to cleave the F-actin accumulated under the cell membrane used for receptor clustering and ruffle formation. Thus, mobilized active cofilin cannot reform into rod-like structures. Similarly, in cells expressing CFL/S3A, the colocalization of cofilin and F-actin at the lamellipodia remained unchanged, suggesting that active cofilin could favor viral entry from cell ruffles. However, a separation of cofilin from F-actin induced by HSV-1 infection at the cell ledge was observed in cells expressing the dominant-negative CFL/S3E. These observations suggest that cofilin may regulate two steps of the entry process and that the alteration of cofilin activity disturbs the coordinated action of two opposite forces during viral binding and penetration. Low concentrations of active cofilin could be involved in F-actin polymerization to facilitate viral binding. Then, the progressive accumulation of active cofilin (reduced phosphorylated cofilin) on the filaments could ultimately favor the disassembly of the actin network promoting viral penetration and intracellular trafficking. In line with this scenario, increasing the pool of active cofilin by expressing the constitutively active S3A cofilin or WT cofilin blocks viral binding and entry presumably due to an excess of depolymerizing activity. Conversely, inactivation by the overexpression of S3E cofilin induces an intense and disorganized accumulation of actin filaments at the cell periphery, preventing viral penetration and thus resulting in the inhibition of virus entry.

In addition, given that cofilin has previously been shown to play a role in the formation of filopodia and lamellipodia (35, 36), we examined the location of p-cofilin in HSV-1-induced filopodia and lamellipodia. Strikingly, the most intense p-cofilin labeling was strongly colocalized within the cell protrusions (Fig. 2E). We also analyzed the effects of cofilin and cofilin mutant expression on the formation of HSV-1-induced ruffles (Fig. 2F). Transient expression of either the wild-type strain or mutants reduced the formation of HSV-1-induced ruffles by 45% $\pm$ 5% compared with expression of nontransfected cells. The knockdown of cofilin expression still reduced the number of filopodia and F-actin accumulation (see Fig. S2D in the supplemental material). We also observed that active cofilin (CFL/S3A) accumulated at the tips of filopodia and local ruffling areas (indicated by an arrow), whereas inactive cofilin (CFL/S3E) did not accumulate during the challenge of HSV-1 stimulation, suggesting a role for cofilin in controlling retrograde filopodia, which may facilitate viral surfing (see Fig. S2E). In addition, we found that another cytoskeletal regulatory protein—LIM and SH3 domain protein 1 (Lasp-1), which regulates cell migration and is involved in HSV-1 infection (37)—has also been involved in HSV-1 entry and virus-induced cell ruffle formation. The overexpression or knockdown of Lasp-1 affects viral entry (see Fig. S3A and B). Because cofilin (Fig. 2E) was localized in ruffles, these proteins are likely to be involved in the HSV-1-mediated ruffling process. In summary, the modulation of cofilin activity plays a critical role in HSV-1 internalization, and an ordered inactivation-activation process of cofilin is exploited by HSV-1. Therefore, either overactivation or inactivation could result in interference with the entry process.

Involvement of RTKs and PI3K in HSV-1 entry and cofilin phosphorylation. Signaling to the cytoskeleton through G protein-coupled receptors, integrins, and receptor tyrosine kinases (RTKs) has been extensively reported to regulate cofilin activity. Moreover, several studies have demonstrated that viral attachment can lead to the activation of host signal transduction cascades, predominantly through tyrosine phosphorylation, which contributes to the internalization of virus into host cells (12, 38). Thus, we tested whether RTKs were involved in HSV-1-induced cofilin phosphorylation. Significantly, genistein, a specific inhibitor of RTKs, inhibited viral entry and cofilin phosphorylation (Fig. 3A). By confocal microscopy, we observed that viral binding quickly induced the activation of tyrosine phosphoproteins while active RTKs gathered and relocalized at the cell membrane when virus entered the cells (Fig. 3B). Due to undifferentiating process, some cells might exhibit the epithelial morphology. Additionally, RTKs were recruited to the sites of virus entry and colocalized with viral capsid protein ICP5 (Fig. 3C). HSV-1 infection also induced the tyrosine phosphorylation of several host proteins (data not shown).

Tyrosine phosphorylation has previously been shown to be involved in PI3K activation, which was reported to support the entry of several viruses into cells (39, 40). To investigate whether this signaling pathway is involved in HSV-1 entry and cofilin phosphorylation, we analyzed the effect of virus uptake on the phosphorylation of Akt, the major downstream effector of the PI3K pathway, which is commonly used as a readout of PI3K activation. Akt was phosphorylated as early as 1 min after virus uptake, and impaired viral entry occurred when cells were treated with LY294002, a specific inhibitor of PI3K (Fig. 3D and E). In addition, Src-family kinases, which are involved in regulating changes in the cytoskeleton during the uptake of various invasive pathogens (12, 41, 42), and PI3K were activated early (Fig. 3F). The pretreatment of cells with PP2, a specific inhibitor of Src family kinases, significantly reduced HSV-1 infection (Fig. 3E). Phosphorylated Src kinases were accumulated at the cell edges early at 5 mpi and were colocalized with viral particles (Fig. 3G), further highlighting the importance of Src-family kinase activity in receptor-induced signaling transduction. In addition, confocal analysis revealed an increased association between tyrosine phosphoproteins and Src during HSV-1 infection but no colocalization between PI3K and Src kinase, which suggests that phosphotyrosine kinases may be the direct upstream kinases that activated PI3K (Fig. 3H). The RTK inhibitor genistein also impaired HSV-1-induced PI3K activation (Fig. 3A). These results suggest that HSV-1 induced cofilin phosphorylation through RTK activation and that PI3K/Akt activation was involved in HSV-1 entry.

EGFR promotes HSV-1-induced early cofilin phosphorylation through PI3K-Akt signaling. Because EGFR, the direct upstream kinase of PI3K, is a member of the RTK family and several studies have demonstrated that EGFR is a critical receptor for hepatitis C virus, influenza A virus, and human cytomegalovirus entry (43–46), we subsequently investigated the role of EGFR in PI3K signaling and HSV-1 entry. First, we tested whether HSV-1 infection activated EGFR. Within 5 min, EGFR was transiently activated and clustered when HSV-1 was added to the cells (Fig. 4A and B; see also Fig. S4A in the supplemental material). The preincubation of cells with EGF or basic fibroblast growth factor (bFGF) enhanced HSV-1 entry into serum-starved cells, whereas vascular endothelial growth factor (VEGF) had no effect (Fig. 4B; see also Fig. S4B). These data suggest that the direct interaction of EGF with the EGFR ligand-binding domain modu-

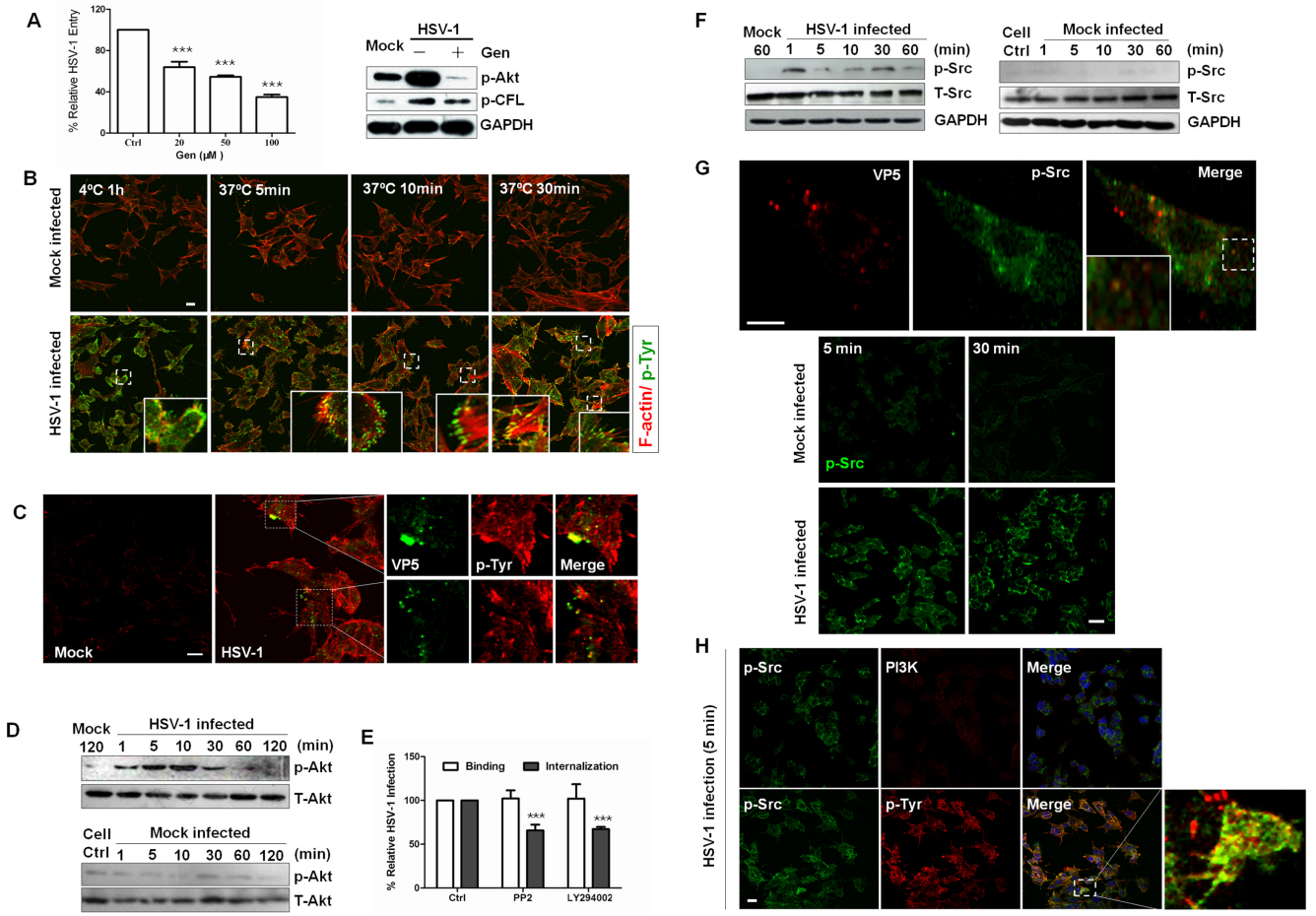

FIG 3 Receptor tyrosine kinases and PI3K are involved in cofilin phosphorylation. (A) Left panel: tyrosine kinase-specific inhibitor genistein (Gen) inhibits HSV-1 entry in a concentration-dependent manner. The cells were pretreated with different concentrations of genistein, and HSV-1 entry was analyzed by quantitative RT-PCR (qRT-PCR). Right panel: Gen inhibited the phosphorylation of Akt and cofilin. The cells pretreated either with or without Gen (100 mM) were exposed to HSV-1, and the cell lysates were probed with the indicated antibodies. (B) Active receptor tyrosine kinases are recruited to the cell membrane at 4°C and dispersed upon virus entry. Monolayer cells that had been infected with HSV-1 or mock infected were stained with anti-p-Tyr at different times. (C) Association of viral particles with pTyr in infected cells. The cells infected with HSV-1 for 5 min were then fixed and processed for double-immunofluorescence analysis using anti-p-Tyr and anti-ICP5 antibodies. (D) Activation of Akt during HSV-1 entry. Active Akt was probed with a p-Akt antibody. (E) Inhibitors prevent HSV-1 entry. The cells were pretreated with PP2 (10 μM) and LY294002 (50 μM) for 1 h. For binding assays, the cells pretreated with inhibitors were incubated with virus (MOI 20) at 4°C for 1 h in the presence of inhibitors, and then the viral DNA was extracted and assayed. (F) Activation of Src family kinases. Active Akt was probed with anti-p-Src (Tyr416) MAb. (G) p-Src is recruited to the cell ledge and colocalizes with ICP5. Upper panels: cells were challenged with HSV-1 for 5 min and were stained with anti-ICP5 MAb (red) and anti-p-Src MAb (green). Lower panels: the cells were infected with HSV-1 or mock infected for 5 min and 30 min and then immunostained with anti-p-Src (Tyr416) MAb (green). (H) pTyr colocalizes with Src in the infected cells. The cells infected with HSV-1 for 30 min were immunostained with anti-p-Tyr and anti-p-Src antibodies and analyzed by confocal microscopy. PI3K staining showed no colocalization with p-Src.

lates HSV-1 entry. To further elucidate the time at which EGFR exerts its effects, we performed a kinetics entry assay using EGFR-specific inhibitor AG-1478 (Fig. 4C; see also Fig. S4C). AG-1478 significantly reduced viral entry at an early stage, before the virus entered the cytoplasm. The binding of HSV-1 (here demonstrated as glycoprotein gB) was also apparently inhibited. These results suggest that EGFR may act as a membrane mediator for entry event initiation and intracellular signaling interchange.

Then, to determine whether HSV initiates viral signaling through EGFR, siRNA was used to assess the role of EGFR in the cofilin phosphorylation signaling pathway. Five siRNAs were tested, and two (SiE4 and SiE5) showed efficient silencing effects (see Fig. S4D in the supplemental material). Both siRNAs reduced viral entry slightly and inhibited the HSV-1-induced Akt and cofilin phosphorylation (Fig. 4D), indicating that EGFR mediated the HSV-1-induced early inactivation of cofilin. We also examined the effect of AG-1478 on Akt and cofilin phosphorylation. The activation of Akt, Src, pTyr, and cofilin phosphorylation was inhibited by 100 nM AG-1478 (Fig. 4E). AG-1478 also blocked EGF-dependent EGFR phosphorylation (Fig. 4F). Additionally, by immunoprecipitation experiments, we found that the interaction between EGFR and PI3K was enhanced by HSV-1 infection and was impaired significantly by AG-1478 treatment (Fig. 4G), which again confirmed the role of EGFR in HSV-1-induced PI3K activation and the subsequent cofilin inactivation and F-actin polymerization. Next, we used other cell lines, including Vero, MRC-5, and HeLa, to determine whether EGFR activation was required for HSV-1 infection. As shown in Fig. S4E, HeLa and

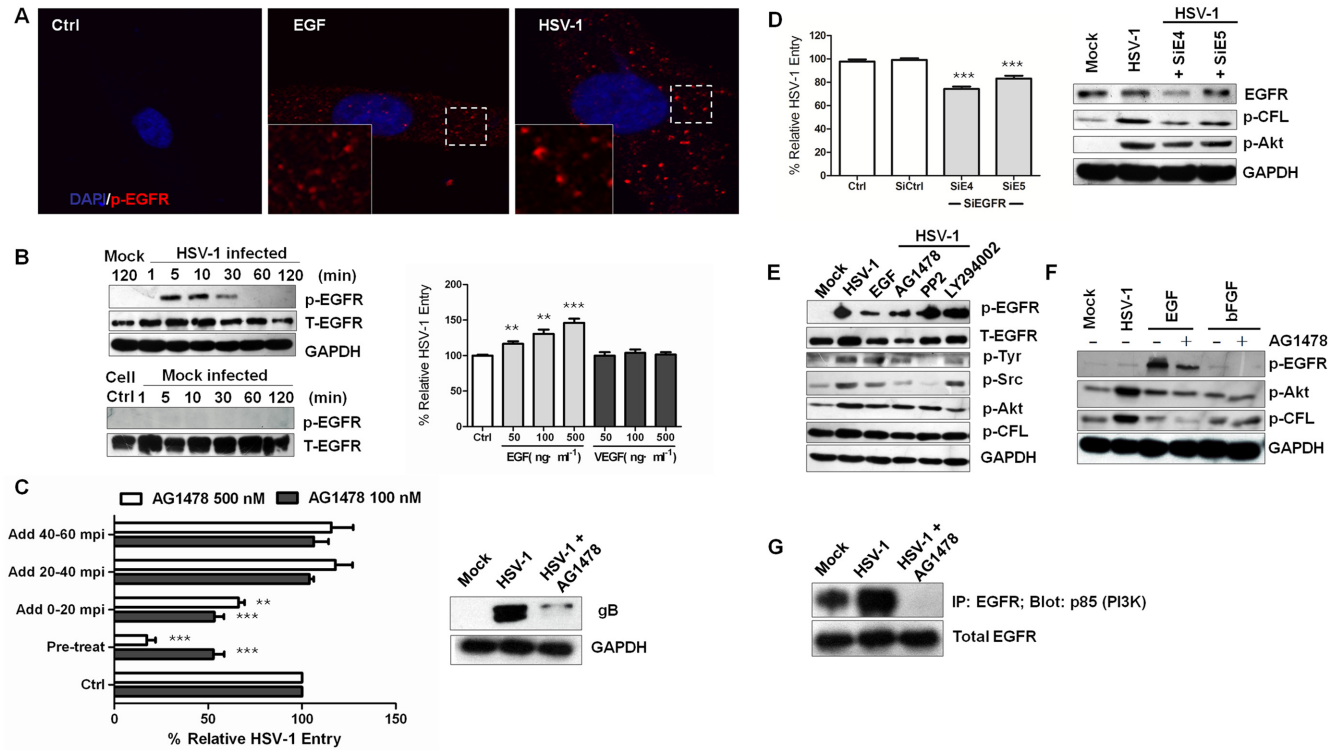

FIG 4 EGFR promotes virus entry and signaling transduction. (A) HSV-1 infection induces EGFR clustering. Cells exposed to HSV-1 for 10 min were stained with anti-p-EGFR antibody. Cells stimulated with EGF (100 ng·ml^{-1}) were used as a control. (B) Activation of EGFR by HSV-1 infection. Left panel: Cell lysates were immunoblotted with anti-p-EGFR and anti-EGFR antibodies. Right panel: the percentages of HSV-1 entry into serum-starved SK–N–SH cells in the presence of EGF or VEGF are shown. VEGF has no effect on HSV-1 entry. The cells were pretreated with EGF, bFGF, or VEGF at different concentrations for 1 h at 37°C. (C) AG-1478 inhibits viral binding. AG-1478 was added at different times, and virus entry was assayed as before. The data are expressed relative to HSV-1 infection without compound. For the experimental setup, see Fig. S5C in the supplemental material. The right panel shows the inhibition of HSV-1 glycoprotein gB binding. Cells infected with HSV-1 for 10 min in the presence or absence of AG-1478 were lysed and probed with an anti-gB antibody. (D) The knockdown of EGFR prevents HSV-1 entry and the phosphorylation of cofilin and Akt. Five siRNAs were used, and siE4 and siE5 inhibited HSV-1 entry. (E) Cross talk between EGFR and PI3K is inhibited by Ly294002 or PP2. The cells were pretreated with AG-1478 (100 nM), PP2 (10 μM), and LY294002 (50 μM) for 1 h before infection. At 10 min after HSV-1 infection, the cell lysates were analyzed for the phosphorylation of EGFR and activation of PI3K. (F) Effect of AG-1478 on EGFR and PI3K activation. AG-1478 blocked EGF-dependent PI3K signaling. Serum-starved SK–N–SH cells were pretreated with either EGF (200 ng·ml^{-1}) or bFGF (200 ng·ml^{-1}) and AG-1478 (100 nM) for 60 min before infection. At 10 min after HSV-1 infection, the cell lysates were analyzed for the activation of EGFR, Akt, and cofilin. (G) AG-1478 reduces the interaction between EGFR and PI3K. Uninfected cells and cells infected with HSV-1 for 10 min in the presence or absence of AG-1478 (100 nM) were lysed and immunoprecipitated (IP) with anti-EGFR and subjected to Western blot analysis with an anti-p85 (PI3K) antibody. The bottom panel shows the blot probed with an anti-EGFR antibody.

Vero cells exhibited enhanced EGFR phosphorylation, suggesting a cell-based EGFR activation. In conclusion, the EGFR-PI3K signaling pathway is involved in HSV-1-mediated early cofilin inactivation and F-actin dynamics.

Lipid rafts are involved in signal coordination. Because EGFR is localized in lipid raft domains (47) and because lipid rafts may function to concentrate the receptors required for binding or inducing signal transduction upon the binding of the viral protein (48–51), we examined whether lipid rafts regulate HSV-1 entry. We examined raft organization in the context of EGF stimulation or viral attachment by labeling the lipid raft marker ganglioside GM1 using fluorescein isothiocyanate (FITC)-conjugated cholera toxin beta subunit (CtxB). In untreated cells, GM1 was detected as an even distribution throughout the cell membrane. However, in cells treated with EGF or HSV-1, GM1 was reorganized to form distinct patches at the membrane, indicating lipid-cluster formation (Fig. 5A). This result is consistent with a previous observation that EGFR is clustered upon virus binding (see Fig. S4A in the supplemental material). Additionally, GM1 was colocalized with viral protein ICP5 during entry (Fig. 5B). Furthermore, methyl-β-cyclodextrin (MβCD) or nystatin, both of which disrupt lipid rafts by removing cholesterol from membranes or sequestering cholesterol out of the plasma membrane, respectively, was able to block HSV-1 infection in a concentration-dependent manner (Fig. 5C). This result indicates that clustering of lipid rafts played an important role in HSV-1 entry, which was consistent with a previous study (51). Notably, although MβCD and nystatin have differential effects on p-Akt and p-CFL, the HSV-1-induced phosphorylation of EFGR was completely inhibited when the cells were incubated with MβCD or nystatin (Fig. 5D). These results suggest an important role for lipid rafts in the regulation of EGFR-PI3K interactions and, therefore, in the coordination of EGFR-dependent signaling pathways.

A role for ERK1/2 in EGFR-PI3K signaling and HSV-1-induced filopodium formation. Because one of the downstream effects of EGFR-PI3K-Rho GTPase activation is the regulation of mitogen-activated protein kinase (MAPK) pathways (52, 53), we next examined whether the EGFR-PI3K signaling pathway re-

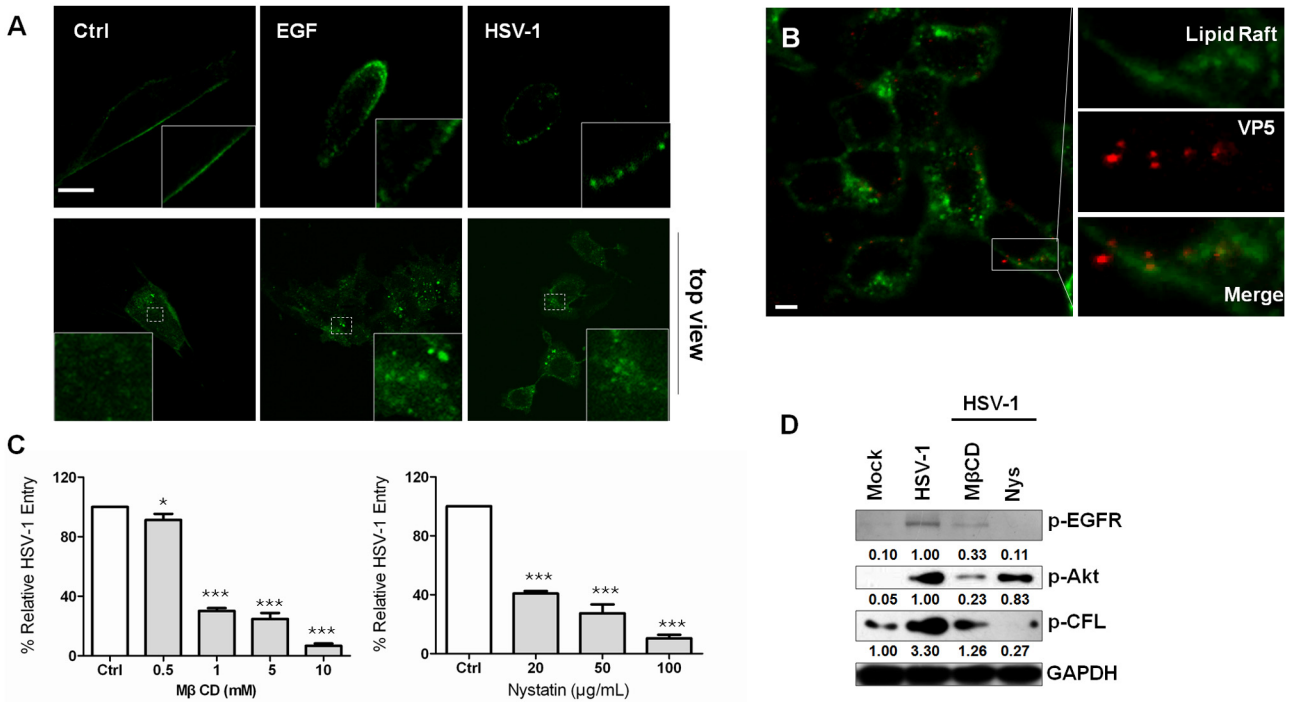

FIG 5 Clustering of lipid rafts is involved in the cofilin phosphorylation signaling cascade. (A) Attachment of HSV-1 causes the clustering of plasma membrane lipids. SK–N–SH cells incubated with the FITC-conjugated cholera toxin beta subunit (CtxB) (30 μg·ml^{-1}) were infected with HSV-1 (MOI 20), stimulated with EGF (100 ng·ml^{-1}), or left untreated for 1 h at 4°C. The samples were then fixed and permeabilized, and images were taken by confocal microscopy. In the top view (lower panels), cells were unpermeabilized and stained with FITC-labeled CtxB under either EGF or HSV-1 stimulation. Scale bar = 10 μm. (B) Viral particles colocalize with lipid rafts. The cells incubated with FITC-conjugated CtxB (green) were bound with HSV-1 for 1 h at 4°C and then incubated at 37°C for 5 min. The samples were fixed and stained with anti-ICP5 antibody (red). (C) Cholesterol-sequestering drugs inhibit HSV-1 infection. The cells were pretreated with the indicated concentrations of methyl-β cyclodextrin or nystatin for 1 h. (D) Lipid raft interruption prevents Akt and Src activation.

quires the ERK pathway to promote cofilin phosphorylation and F-actin polymerization when induced by HSV-1. Enhanced Erk1/2 activity was observed in HSV-1 infection as early as 1 mpi, and a steady increase in HSV-1-induced ERK activation reached its peak activity at 30 mpi (Fig. 6A). The pretreatment of cells with U0126, a potent and specific covalent binding inhibitor of MEK1/2, an upstream kinase of Erk1/2, totally inhibited HSV-1-induced ERK phosphorylation without affecting the total ERK levels (Fig. 6B). Additionally, the treatment with U0126 inhibited HSV-1-induced cofilin phosphorylation and viral entry in a dose-dependent manner without influencing virus binding (Fig. 6C and D). To determine whether PI3K and Src are needed for Erk1/2 activation, kinase inhibitors were used to detect HSV-1-induced Erk1/2 activation (Fig. 6E). Apparently, the activation of Erk1/2 and cofilin phosphorylation were inhibited when the cells were treated with LY294002 and PP2 as well as with U0126, indicating that HSV-1-induced Erk1/2 activation is dependent on EGFR-PI3K activity. Specifically, Src inhibitor PP2 inhibited Akt activation (Fig. 6E), indicating that Src kinase is an upstream kinase of PI3K. This result was corroborated by the recent finding that HSV-1 VP11/12 recruited Src kinase Lck to initiate signaling through the PI3K/Akt signaling module (54).

In addition, using confocal analysis, we found that during the early infection of HSV-1, activated Erk1/2 increased and was recruited to the base of filopodia (Fig. 6F). These results indicate a possible role for Erk1/2 in controlling virus-induced filopodium formation and retrograde actin by regulating cofilin activity, which promoted virus surfing and binding when differential rates of actin polymerization in the filopodia and cell cortex occurred (55). In addition, Erk1/2 activation influenced the formation of filopodia. Cells treated with U0126 possessed a distinct morphology and markedly fewer filopodia, with a 4-fold decrease (Fig. 6G). Furthermore, Erk1/2 is reported to regulate the activity of myosin II by inducing the indirect phosphorylation of the myosin light chain (MLC) (56). When cells were infected with HSV-1, phosphorylated MLC was activated and located at the base of filopodia, indicating that myosin II was also involved in HSV-1-induced filopodium formation (Fig. 6H). Moreover, inhibitors prevented HSV-1-induced MLC activation (Fig. 6E). Taken together, these results indicate that EGFR-PI3K activation is the upstream event leading to MEK-ERK activation by HSV-1 and that Erk1/2 controls early cofilin phosphorylation and virus-induced filopodium formation.

ROCK is downstream of ERK1/2 in the early cofilin phosphorylation. Erk1/2-controlled cofilin phosphorylation had previously been reported to occur through Rho-associated, coiled-coil-containing protein kinase 1 (ROCK), a Rho kinase that phosphorylates and activates LIMK (57, 58). Besides, entry of equine herpesvirus 1 was demonstrated to depend upon the activation of ROCK1 (59). As expected, ROCK was activated, and its specific inhibitor Y27632 inhibited HSV-1 entry (Fig. 7A). We also tested the activation of p21-activated kinase (PAK), another Rho GTPase kinase that directly phosphorylates LIMK. PAK is activated by RAC1 or CDC42 and is associated with cytoskeleton re-

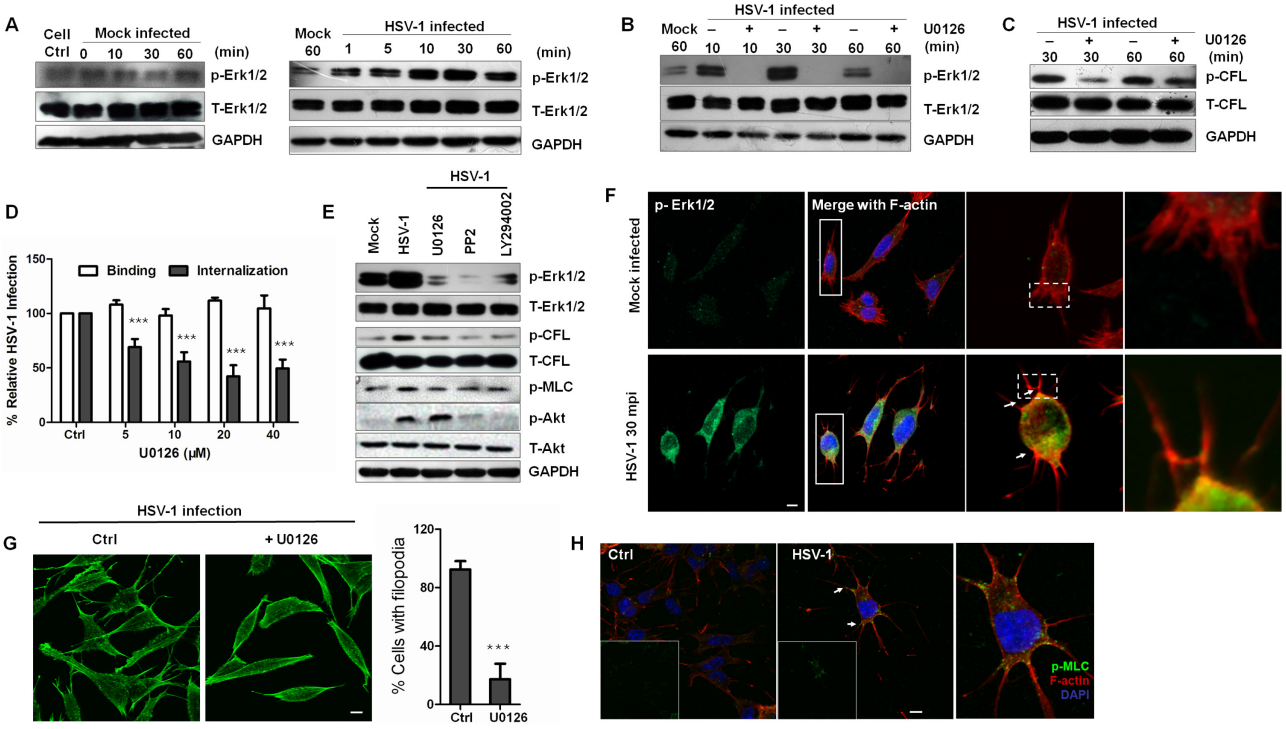

FIG 6 Erk1/2 activation controls EGFR-mediated cofilin phosphorylation and virus-induced filopodia. (A) Kinetics of Erk1/2 induction during HSV-1 early infection. Cell lysates were immunoblotted with anti-p-Erk1/2 MAb and anti-Erk1/2 antibodies. Cells of the mock group were placed at 4°C for 1 h and transferred to 37°C for 0, 10, 30, and 60 min. (B to D) The inhibition of MEK1/2 inhibits Erk1/2 activity (B), cofilin phosphorylation (C), and virus entry (D). The cells were either mock infected or infected with HSV-1 in the presence or absence of U0126 (20 μM) for different times. (E) PI3K or Src kinase is the upstream kinase of Erk1/2. The cells pretreated with PP2 (10 μM), LY294002 (50 μM), or U0126 (20 μM) were mock infected or infected with HSV-1 for 30 min, lysed, and then probed with different antibodies. (F) Recruitment of active Erk1/2 to the base of the filopodia. The cells exposed to HSV-1 or not at the indicated time were stained with anti-p-Erk1/2 (green) and TRITC-phalloidin (red). Arrows indicate the colocalization of active Erk1/2 with F-actin at the base of filopodia. (G) Erk1/2 inhibition reduces the HSV-1-mediated production of filopodia. The cells exposed to HSV-1 in the presence or absence of U0126 (20 μM) for 30 min at 37°C were examined. The graph quantifies the effect of U0126 on filopodium formation. At least 100 cells from five representative fields were counted in each experiment. (H) MLC is activated and recruited to the base of the filopodia (arrows). The cells were infected for 60 min and stained with anti-p-MLC MAb (green) or F-actin (red).

organization. During HSV-1 infection, no obvious change occurred, and IPA-3, an irreversible inhibitor that prevents PAK activation, had no impact on viral infection or binding (Fig. 7B). These results suggest that PAK activation is not involved in the HSV-1-induced phosphorylation of LIMK. Moreover, PI3K and Src inhibitors and an Erk1/2 inhibitor inhibited virus-induced ROCK activation, whereas none of these inhibitors altered the phosphorylated PAK/total PAK expression levels (Fig. 7C). In addition, we explored the role of another cytoskeleton regulator—the Arp2/3 complex—in HSV-1 entry using its specific inhibitor CK-548. Arp2/3 can nucleate actin filaments, cap their pointed ends, and cross-link them into orthogonal networks. Arp2/3 always localizes to membrane ruffles and dynamic regions of the actin assembly. However, the treatment with CK-548 did not prevent HSV-1 entry, binding, or postentry (Fig. 7D). In summary, the results described above indicate that HSV-1 induced early cofilin phosphorylation through a signaling pathway, such as the EGFR-PI3K-Erk1/2-ROCK pathway, which is illustrated as a simple schematic diagram in Fig. 7E.

DISCUSSION

Although actin reorganization in the presence of HSV-1 had been reported in several cell systems (5), the mechanism and functional consequences of this phenomenon have remained largely uncertain, especially regarding the process of entry of HSV-1 into neuronal cells. In this study, we identified cofilin as a critical factor required for HSV-1 infection. HSV-1 entry required a two-phase process of rapid actin polymerization and depolymerization events, and HSV-1-triggered cofilin activity is regulated in a biphasic manner (Fig. 8): viral binding induced the phosphorylation of cofilin via EGFR-PI3K-Erk1/2-ROCK-LIMK signals for F-actin polymerization and efficient entry, and subsequent viral penetration activated cofilin, leading to the fragmentation of existing actin filaments, and also, presumably, loosening of the actin cortex and facilitation of virus trafficking. These findings strongly suggest that HSV-1 has evolved infection strategies to tightly modulate virus entry by regulating cofilin activity and inducing dynamic actin polymerization and depolymerization.

F-actin regulation plays a critical role in neuron function, and the modulation of F-actin dynamics or relevant regulators might result in the disruption of cellular functions or in the occurrence of neurological diseases (60). Cofilin, as one of the actin regulators, has been shown to be related in neurodegenerative processes (61). Previously, cofilin activity regulation was shown to be involved in virus-mediated actin remodeling (62–64), and our previous work demonstrated that cofilin also participated in HSV-1

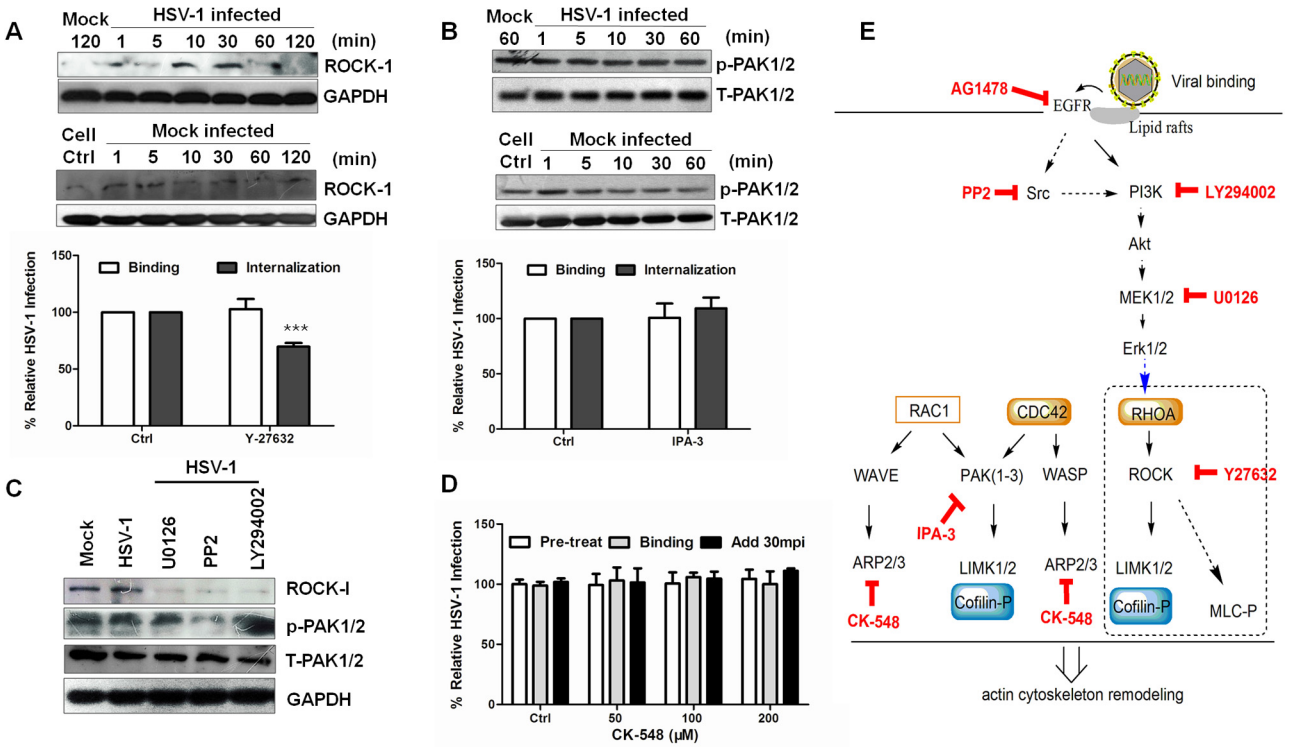

FIG 7 ROCK is a downstream effector of Erk1/2 in HSV-1-induced early cofilin phosphorylation. (A) ROCK activation during HSV-1 entry. The cells were infected with HSV-1 (MOI 20), and the cell lysates were analyzed with an anti-ROCK antibody. The ROCK inhibitor, Y-27632 (100 μM), was used to confirm its effect on HSV-1 entry. (B) PAK1/2 is not involved in HSV-1 entry, and the PAK1/2-specific inhibitor IPA-3 (20 μM) did not affect virus entry or binding. (C) Kinase inhibitors block the activation of ROCK with no effect on PAK1/2. Inhibitor concentrations were similar to those used before. (D) Arp2/3 complex inhibitor CK548 does not affect HSV-1 entry, binding, or postentry. (E) Simple schematic of the signaling pathway involved in HSV-1-induced early cofilin phosphorylation.

infection and replication (7, 37). We show here that the cofilin phosphocycle is critical for efficient virus entry and that both the downregulation and upregulation of cofilin activity inhibited HSV-1 internalization (Fig. 2). Dynamic cofilin activity affected the formation of virus-mediated cell ruffles, and tight control of the local concentration of active cofilin is essential for actin-dependent processes such as receptor clustering and intracellular migration. Interestingly, pathogens, such as HIV and other invasive pathogens, also modulate their uptake into host cells by controlling cofilin activity and actin rearrangement (34, 65–67). During HIV-1 infection, $G\alpha_i$-dependent signaling from the CXCR4 chemokine coreceptor was utilized by active cofilin for viral nuclear localization (67). Based on these observations, we postulate that by regulating actin cytoskeleton dynamics, cofilin biphasic activation could present an example of specific cellular machinery being usurped by a pathogen.

Our results suggest that the HSV-1-induced EGFR-PI3K signaling pathway actively participates in the early entry steps. The engagement of RTKs is a major mechanism that transforms extracellular signaling into intracellular kinases and a cytoskeleton response. EGFR is a well-studied member of the RTK family and is involved in the uptake of several viruses (41–44). In our experiments, EGFR was not only clustered upon HSV-1 attachment (Fig. 3B) but was also activated, promoting the activation of downstream kinases (Fig. 4). Similarly to the case of EGF, HSV-1 infection induced the aggregation of lipid rafts, gathering a concentration of signaling molecules within the clustered lipid rafts and thereby initiating signal transduction and HSV-1 internalization. When cells were treated with lipid raft-specific inhibitors, viral entry was significantly inhibited (51). Moreover, EGFR inhibitor and siRNAs block HSV-1 infection by inhibiting downstream signaling cascades (Fig. 4D and E), whereas the EGFR ligand EGF enhances HSV-1 entry kinetics potentially by inducing the redistribution and internalization of HSV-1 entry receptors (Fig. 4B). Interestingly, the internalization of influenza A virus activated EGFR via the clustering of lipid rafts, suggesting that EGFR internalization may be a common mechanism utilized by viruses to enter cells. Further investigation will be required to identify which viral protein induces EGFR clustering and whether other possible coreceptors are involved in viral signaling and entry.

Kinases, such as PI3K and Erk1/2, are well-known downstream effectors of EGFR. Although the activity of Erk1/2 and PI3K kinases has been associated with several virus internalization processes (48, 49, 68, 69), the upstream targets and effectors of these kinases have not been described in detail and are not known to be important for HSV-1 infection. Tiwari and Shukla reported that PI3K may affect multiple steps during HSV-1 entry into human conjunctival epithelial cells (69). However, the specific viral and cellular mediators of HSV-1-activated PI3K remain to be elucidated. Furthermore, a limited number of studies have focused on the role for Erk1/2 in HSV-1 life cycles (70, 71), and they all showed that HSV-1 replication required the suppression of ERK activity. No study had been performed to investigate whether

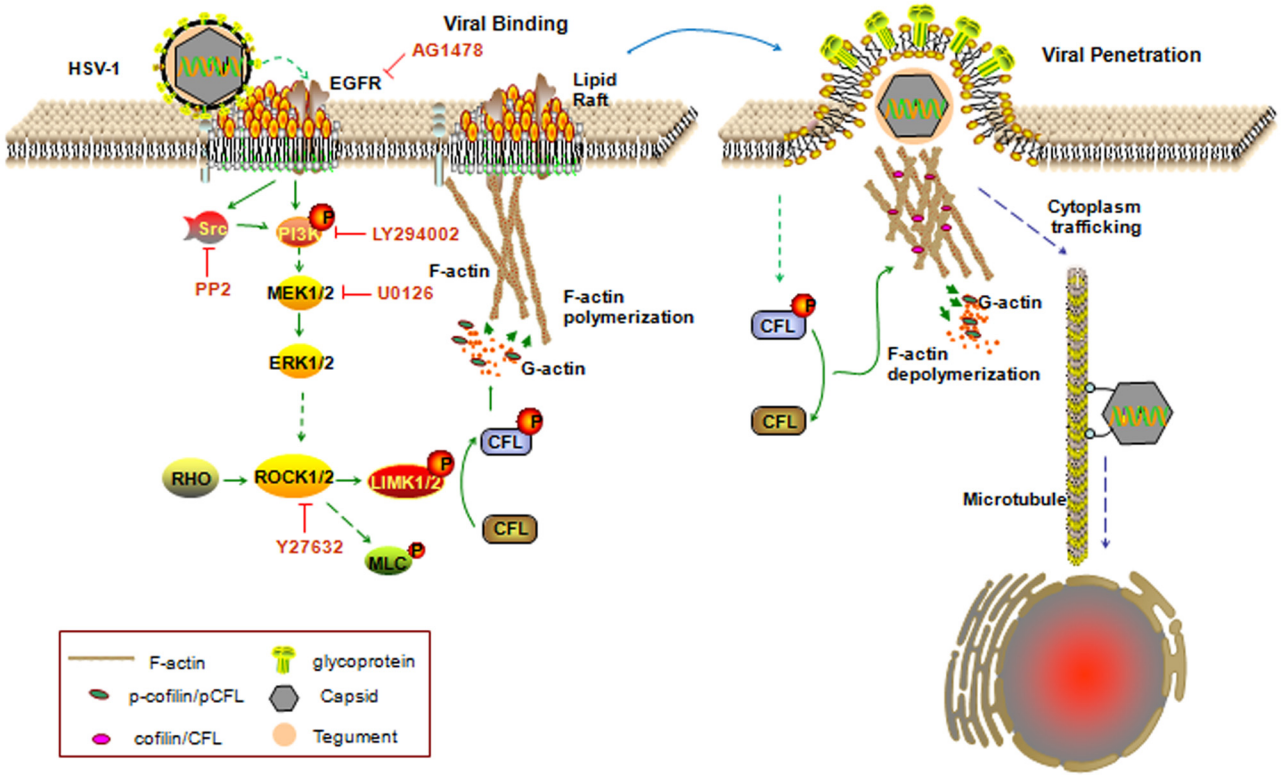

FIG 8 Model of cofilin regulating actin dynamics and initiating HSV-1 entry. During early infection, the virus induces cofilin inactivation and F-actin polymerization via the EGFR-PI3K-Erk1/2-ROCK-LIMK signaling pathway, which may promote receptor clustering and initiate the entry process. Lipid rafts are clustered and serve as signaling platforms for EGFR-mediated cofilin inactivation. Subsequent viral penetration requires F-actin depolymerization through cofilin activation. Thus, the biphasic activation of cofilin represents specific cellular machinery usurped by HSV-1.

Erk1/2 is involved in HSV-1 entry. We found that both PI3K and Erk1/2 kinases mediated signaling transduction from cell membrane receptors to intracellular actin remodeling in a PI3K-Erk1/2 sequence. Moreover, because Erk1/2 was localized at the base of filopodia (Fig. 6F), Erk1/2 may control filopodium formation and retraction, which promotes virus surfing and binding when differential rates of actin polymerization occur in the filopodia and cell cortex. Additionally, we established that there is a critical role of Src kinase and phosphorylated tyrosine kinases in HSV-1 entry. The activation of Src-family kinases allows for the activation of EGFR-PI3K-Erk1/2-ROCK-LIMK-cofilin signaling. These results confirm and extend the implication of EGFR in HSV-1 infection and identify both EGFR inhibitors and ROCK inhibitors as potential HSV-1-inhibitory drugs (59). In addition, the inhibition of myosin light-chain phosphorylation, another ROCK-regulated process, might inhibit virus entry, which is in accord with recent evidence showing that the inhibition of myosin light-chain kinase and nonmuscle myosin IIA can be targeted for the development of new therapies against HSV-1 (72).

Our results also strongly indicate that EGFR-PI3K activation promotes the RhoA-ROCK signaling pathway to inactivate cofilin and regulate F-actin but that neither Cdc42 nor Rac1 has an effect on virus entry (Fig. 7). A cell-type-specific intermediate pathway is engaged during HSV-1 entry into different host cells. Specifically, binding to different receptors leads to the activation of different Rho GTPases. For example, during HSV-1 entry into MDCKII cells, Cdc42 and Rac1, but not RhoA, were activated and vice versa during entry in primary corneal fibroblasts and nectin-1-overexpressing CHO cells (9, 10). However, the specific and direct actin regulatory component downstream of Rho GTPase was not confirmed in those studies.

In summary, our results define the specific mechanism of cytoskeleton remodeling during HSV-1 entry into neurons, which could lead to a greater understanding of viral entry and pathogenesis of HSV-1-induced neurological diseases or help the development of more efficient oncolytic virotherapy. We emphasize that cofilin activity regulation acts as a molecular switch to provide a functional link between cytoskeleton rearrangement and the viral entry process. Thus, both the surface receptors and upstream signaling molecules are viable targets for the development of therapeutic antiviral strategies.

MATERIALS AND METHODS

Cells and virus. The sources and culture conditions for different cell lines have been previously described (7, 37). The neuroblastoma cell line SK–N–SH (ATCC HTB-11), purchased from the cell bank of the Chinese Academy of Sciences, was propagated in Eagle's minimal essential medium (MEM) (Invitrogen) supplemented with 10% fetal bovine serum (FBS) (Invitrogen), 1.0 mM sodium pyruvate (Sigma), 0.1 mM nonessential amino acids (Invitrogen), and 1.5 g/liter sodium bicarbonate (Sigma). HSV-1 strain F (ATCC VR733), obtained from Hong Kong University, was propagated in Vero cells and stored at −80°C until use. All cells were purchased from ATCC.

Antibodies, small-compound inhibitors, siRNAs, and plasmids. Site-directed mutagenesis was carried out to construct CFL mutants using

a QuikChange site-directed mutagenesis kit (Stratagene, La Jolla, CA). All constructs were verified by DNA sequencing. For a full list of the antibodies, inhibitors, plasmids, siRNAs, and reagents used, please refer to Tables S1 to S6 in the supplemental material. All inhibitors were used at a noncytotoxic concentration. The cytotoxicity of chemical inhibitors and siRNA and transient expression were determined with a MTT [3-(4,5-dimethyl-2-thiazolyl)-2,5-diphenyl-2H-tetrazolium bromide] assay.

Flow cytometry. Flow cytometry (FCM) was used to quantify F-actin reorganization. Briefly, cells were washed with phosphate-buffered saline (PBS) and fixed for 5 min in 4% formaldehyde–PBS. After being washed extensively with PBS, the cells were permeabilized with 0.1% Triton X-100–PBS and washed again with PBS. The cells were then stained with 5% M fluorescein isothiocyanate (FITC)–phalloidin (Sigma-Aldrich)–PBS for 40 min, and the unbound phalloidin conjugate was removed by several washes with PBS. The fluorescence was then analyzed with an flow cytometer (Becton Dickinson).

Measurement of HSV-1 entry. Viral entry was detected as described previously (7, 33, 73). Briefly, cells were seeded 24 h prior to experimentation in 12-well or 24-well plates. The cells were pretreated with inhibitors at 37°C for different times, and then HSV-1 (multiplicity of infection [MOI] = 20) binding to cells was performed for 1 h at 4°C in the absence of inhibitors. Then, the cells were washed with PBS (pH 3.0) to remove the bound but not entered virions and incubated at 37°C with the indicated compounds for 1 h. The cells were then washed three times with PBS and digested and recovered by centrifugation, and the internalized viral DNA was isolated using a UNIQ-10 viral DNA kit (Sangon; China). HSV-1 infection and entry were assessed by detecting the viral UL47 gene and UL46 gene using real-time DNA PCR and were expressed relative to control infections without the addition of inhibitors. The PCR amplification product of UL46/UL47 was purified using Gel Extraction Kit II (U-gene; China), diluted serially, and used as a standard for quantitative analysis. The initial copy number of UL46/UL47 DNA in each group was calculated using the following formula: $C_T = -K \log X0 + b$, where C_T is the cycle threshold and K, $X0$, and b refer to the slope rate, initial copy number, and constant, respectively. For the HSV-1 binding assay, cells were incubated with virus in the presence of inhibitors at 4°C for 1 h, and then cells were washed to remove unbounded virus. Total viral DNA was extracted and measured by real-time PCR. To study the EGFR effect on HSV-1 entry, AG-1478 inhibitor was added every 20 min after viral binding. To assess the effect of EGF on HSV-1 entry, serum-starved SK–N–SH cells were preincubated in serum-free medium in the presence or absence of EGF prior to HSV-1 binding and entry in the presence or absence of EGF. For the mRNA expression level assay, total RNA was extracted with TRIzol reagent (Invitrogen), and 1 μg of RNA was then reverse transcribed with a PrimeScript RT reagent kit (TaKaRa).

Penetration assay. A plaque assay was performed to measure the penetration rate (7). Monolayers of Vero cells were chilled to 4°C for 1 h prior to infection with 300 PFU of virus. The dishes were incubated at 4°C for 1 h to allow virus adsorption and then transferred to 37°C, and at various times ranging from 0 to 120 min, the monolayers were washed with a pH 3 citrate buffer before being overlaid with medium containing 1% human serum.

Western blotting. Cells were lysed in radioimmunoprecipitation assay (RIPA) buffer (15 mM NaCl, 1 mM $MgCl_2$, 1 mM $MnCl_2$, 2 mM $CaCl_2$, 2 mM phenylmethylsulfonyl fluoride, phosphatase inhibitor cocktail S [Invitrogen]). The lysates were normalized to equal amounts of protein, and the proteins were separated by SDS-PAGE (7.5% to 12.5% gradient), transferred to nitrocellulose, and probed with the indicated primary antibodies. Detection was conducted by incubation with species-specific horseradish peroxidase (HRP)-conjugated secondary antibodies. Immunoreactive bands were visualized by enhanced chemiluminescence (Beyotime; China). ImageJ software was used to quantify the band intensity. For each point, the signal intensity for each protein was normalized to the signal intensity measured for GAPDH (glyceraldehyde-3-phosphate dehydrogenase) and was expressed as the fold increase relative to the control.

Immunoprecipitation. Cell lysates were preincubated with 1.0 μg of appropriate control IgG and 20 μl of protein A/G Plus-agarose at 4°C for 30 min. Then, supernatants were incubated for 1 h with immunoprecipitating antibody at 4°C, and the immune complexes were captured by protein A/G Plus-agarose at 4°C overnight. The samples were assayed by Western blotting with specific primary and secondary antibodies.

Transfection and transient expression. For siRNA knockdowns and plasmid overexpression, cells were transfected as described previously. The cells were plated the day before at a density of 10^5 cells or at 50% to 60% confluence per well, transfected with Lipofectamine LTX and Plus reagents (Invitrogen) for plasmids or with Lipofectamine 2000 reagent (Invitrogen) for siRNA according to the manufacturer's instructions, and incubated for 24 h.

Immunofluorescence staining and analysis. Cells were challenged with virus at 4°C for 1 h and then incubated at 37°C for the times indicated. Samples were washed in PBS, fixed in 4% paraformaldehyde (PFA)–PBS for 15 min, and permeabilized with 0.1% Triton X-100 for 5 min. The samples were blocked in 5% bovine serum albumin (BSA) and incubated with primary antibodies (1:1,000 for the Cell Signaling Technology [CST] antibody and 1:3,000 for the Abcam antibody) and fluorochrome-conjugated secondary antibodies (1:1,000). Unless otherwise specified, stainings were performed at room temperature for 1 h. Additionally, 5 μM tetramethyl rhodamine isocyanate (TRITC)–phalloidin (Sigma) was added for 40 min and 1 mg/ml DAPI (4′,6′ diamidino-2-phenylindole)–PBS was added for 15 min to label F-actin and nuclei, respectively. Images were captured with a Zeiss LSM510 Meta confocal system under a 63× oil immersion objective (Carl Zeiss). The fluorescence intensity of the images was processed and quantified using ImageJ software. Also, the colocalization of two channels was detected using the colocalization finder plug-in.

To copatch lipid rafts with the proteins of interest and for colocalization experiments, cells were incubated with HSV-1, FITC-conjugated cholera toxin beta subunit (CtxB) (Invitrogen) was added at 4°C for 1 h, and the cells were subsequently shifted to 37°C for the time indicated to visualize raft-resident ganglioside M1 (GM1). Proteins of interest were visualized using a common immunofluorescence staining protocol, and images were taken by confocal microscopy.

Effects of cofilin mutation on viral entry were evaluated as previously described (7), using a method similar to that in a previous report (74). Briefly, SK–N–SH cells with 40% to 50% confluence were transfected with plasmids and then infected with HSV-1 for 1 h. Then, cells were stained with primary antibody against HSV-1 (ICP5; 1:3,000). F-actin and nuclei were stained as described above. Images were acquired by laser scanning microscopy (LSM) for 5 fields of view per dish to enable the counting of ICP5-positive capsids docked at nuclei. The average number of ICP5-positive capsids per nuclei and the percentage of positive nuclei (nuclei docked with at least 1 ICP5-positive capsid) were calculated to evaluate the viral entry.

Statistical analysis. Student's two-tailed t test was used for all statistical analysis, with the levels of significance set at $P < 0.0005$ (represented with three asterisks [***] in the figures), $P < 0.005$ (**), and $P < 0.05$ (*).

SUPPLEMENTAL MATERIAL

Supplemental material for this article may be found at http://mbio.asm.org/lookup/suppl/doi:10.1128/mBio.00958-13/-/DCSupplemental.

Figure S1, TIF file, 12.3 MB.
Figure S2, TIF file, 2.9 MB.
Figure S3, TIF file, 4.6 MB.
Figure S4, TIF file, 2.9 MB.
Table S1, DOCX file, 0 MB.
Table S2, DOCX file, 0.1 MB.
Table S3, DOCX file, 0.1 MB.

Table S4, DOCX file, 0.1 MB.
Table S5, DOCX file, 0.1 MB.
Table S6, DOCX file, 0.1 MB.

ACKNOWLEDGMENTS

We thank Genepharma Co. Ltd. (Shanghai, China) for the supply of siRNAs.

This work was supported by the twelfth 5-year National Science and Technology Support Program (2012BAI29B06), the National Natural Science Foundation of China (81274170), and the Foundation for High-level Talents in Higher Education of Guangdong, China (2010; no. 79).

REFERENCES

1. **MacLeod IJ, Minson T.** 2010. Binding of herpes simplex virus type-1 virions leads to the induction of intracellular signalling in the absence of virus entry. PLoS One **5:**e9560. http://dx.doi.org/10.1371/journal.pone.0009560.
2. **Salameh S, Sheth U, Shukla D.** 2012. Early events in herpes simplex virus lifecycle with implications for an infection of lifetime. Open Virol. J. **6:**1–6. http://dx.doi.org/10.2174/1874357901206010001.
3. **Lyman MG, Enquist LW.** 2009. Herpesvirus interactions with the host cytoskeleton. J. Virol. **83:**2058–2066. http://dx.doi.org/10.1128/JVI.01718-08.
4. **Taylor MP, Koyuncu OO, Enquist LW.** 2011. Subversion of the actin cytoskeleton during viral infection. Natl. Rev. Microbiol. **9:**427–439. http://dx.doi.org/10.1038/nrmicro2574.
5. **Roberts KL, Baines JD.** 2011. Actin in herpesvirus infection. Viruses **3:**336–346. http://dx.doi.org/10.3390/v3040336.
6. **Shukla D, Spear PG.** 2001. Herpesviruses and heparan sulfate: an intimate relationship in aid of viral entry. J. Clin. Invest. **108:**503–510. http://dx.doi.org/10.1172/JCI200113799.
7. **Xiang Y, Zheng K, Ju H, Wang S, Pei Y, Ding W, Chen Z, Wang Q, Qiu X, Zhong M, Zeng F, Ren Z, Qian C, Liu G, Kitazato K, Wang Y.** 2012. Cofilin 1-mediatee biphasic F-actin dynamics of neuronal cells affect herpes simplex virus 1 infection and replication. J. Virol. **86:**8440–8451. http://dx.doi.org/10.1128/JVI.00609-12.
8. **Hoppe S, Schelhaas M, Jaeger V, Liebig T, Petermann P, Knebel-Mörsdorf D.** 2006. Early herpes simplex virus type 1 infection is dependent on regulated Rac1/Cdc42 signalling in epithelial MDCKII cells. J. Gen. Virol. **87:**3483–3494. http://dx.doi.org/10.1099/vir.0.82231-0.
9. **Petermann P, Haase I, Knebel-Mörsdorf D.** 2009. Impact of Rac1 and Cdc42 signaling during early herpes simplex virus type 1 infection of keratinocytes. J. Virol. **83:**9759–9772. http://dx.doi.org/10.1128/JVI.00835-09.
10. **Rahn E, Petermann P, Hsu MJ, Rixon FJ, Knebel-Mörsdorf D.** 2011. Entry pathways of herpes simplex virus type 1 into human keratinocytes are dynamin- and cholesterol-dependent. PLoS One **6:**e25464. http://dx.doi.org/10.1371/journal.pone.0025464.
11. **Clement C, Tiwari V, Scanlan PM, Valyi-Nagy T, Yue BY, Shukla D.** 2006. A novel role for phagocytosis-like uptake in herpes simplex virus entry. J. Cell Biol. **174:**1009–1021. http://dx.doi.org/10.1083/jcb.200509155.
12. **Coyne CB, Bergelson JM.** 2006. Virus-induced Abl and Fyn kinase signals permit coxsackievirus entry through epithelial tight junctions. Cell **124:**119–131. http://dx.doi.org/10.1016/j.cell.2005.10.035.
13. **Lehmann MJ, Sherer NM, Marks CB, Pypaert M, Mothes W.** 2005. Actin- and myosin-driven movement of viruses along filopodia precedes their entry into cells. J. Cell Biol. **170:**317–325. http://dx.doi.org/10.1083/jcb.200503059.
14. **Steffens CM, Hope TJ.** 2004. Mobility of the human immunodeficiency virus (HIV) receptor CD4 and coreceptor CCR5 in living cells: implications for HIV fusion and entry events. J. Virol. **78:**9573–9578. http://dx.doi.org/10.1128/JVI.78.17.9573-9578.2004.
15. **Jiménez-Baranda S, Gómez-Moutón C, Rojas A, Martínez-Prats L, Mira E, Ana Lacalle R, Valencia A, Dimitrov DS, Viola A, Delgado R, Martinez-A C, Mañes S.** 2007. Filamin-A regulates actin-dependent clustering of HIV receptors. Nat. Cell Biol. **9:**838–846. http://dx.doi.org/10.1038/ncb1610.
16. **Barrero-Villar M, Cabrero JR, Gordón-Alonso M, Barroso-González J, Alvarez-Losada S, Muñoz-Fernández MA, Sánchez-Madrid F, Valenzuela-Fernández A.** 2009. Moesin is required for HIV-1-induced CD4-CXCR4 interaction, F-actin redistribution, membrane fusion and viral infection in lymphocytes. J. Cell Sci. **122:**103–113. http://dx.doi.org/10.1242/jcs.035873.
17. **Chandran B.** 2010. Early events in Kaposi's sarcoma-associated herpesvirus infection of target cells. J. Virol. **84:**2188–2199. http://dx.doi.org/10.1128/JVI.01334-09.
18. **Zambrano A, Solis L, Salvadores N, Cortés M, Lerchundi R, Otth C.** 2008. Neuronal cytoskeletal dynamic modification and neurodegeneration induced by infection with herpes simplex virus type 1. J. Alzheimers Dis. **14:**259–269.
19. **Nishita M, Tomizawa C, Yamamoto M, Horita Y, Ohashi K, Mizuno K.** 2005. Spatial and temporal regulation of cofilin activity by LIM kinase and slingshot is critical for directional cell migration. J. Cell Biol. **171:**349–359. http://dx.doi.org/10.1083/jcb.200504029.
20. **Popow-Woźniak A, Mazur AJ, Mannherz HG, Malicka-Błaszkiewicz M, Nowak D.** 2012. Cofilin overexpression affects actin cytoskeleton organization and migration of human colon adenocarcinoma cells. Histochem. Cell Biol. **138:**725–736. http://dx.doi.org/10.1007/s00418-012-0988-2.
21. **Biedler JL, Roffler-Tarlov S, Schachner M, Freedman LS.** 1978. Multiple neurotransmitter synthesis by human neuroblastoma cell lines and clones. Cancer Res. **38:**3751–3757.
22. **Ross RA, Biedler JL, Spengler BA.** 2003. A role for distinct cell types in determining malignancy in human neuroblastoma cell lines and tumors. Cancer Lett. **197:**35–39. http://dx.doi.org/10.1016/S0304-3835(03)00079-X.
23. **Abemayor E, Sidell N.** 1989. Human neuroblastoma cell lines as models for the *in vitro* study of neoplastic and neuronal cell differentiation. Environ. Health Perspect. **80:**3–15. http://dx.doi.org/10.1289/ehp.89803.
24. **Nicola AV, Hou J, Major EO, Straus SE.** 2005. Herpes simplex virus type 1 enters human epidermal keratinocytes, but not neurons, via a pH-dependent endocytic pathway. J. Virol. **79:**7609–7616. http://dx.doi.org/10.1128/JVI.79.12.7609-7616.2005.
25. **Orvedahl A, Alexander D, Tallóczy Z, Sun Q, Wei Y, Zhang W, Burns D, Leib DA, Levine B.** 2007. HSV-1 ICP34.5 confers neurovirulence by targeting the Beclin 1 autophagy protein. Cell Host Microbe **1:**23–35. http://dx.doi.org/10.1016/j.chom.2006.12.001.
26. **Quattrocchi S, Ruprecht N, Bönsch C, Bieli S, Zürcher C, Boller K, Kempf C, Ros C.** 2012. Characterization of the early steps of human parvovirus B19 infection. J. Virol. **86:**9274–9284. http://dx.doi.org/10.1128/JVI.01004-12.
27. **Schmidt FI, Bleck CK, Helenius A, Mercer J.** 2011. Vaccinia extracellular virions enter cells by macropinocytosis and acid-activated membrane rupture. EMBO J. **30:**3647–3661. http://dx.doi.org/10.1038/emboj.2011.245.
28. **Dixit R, Tiwari V, Shukla D.** 2008. Herpes simplex virus type 1 induces filopodia in differentiated P19 neural cells to facilitate viral spread. Neurosci. Lett. **440:**113–118. http://dx.doi.org/10.1016/j.neulet.2008.05.031.
29. **Galdiero M, Whiteley A, Bruun B, Bell S, Minson T, Browne H.** 1997. Site-directed and linker insertion mutagenesis of herpes simplex virus type 1 glycoprotein H. J. Virol. **71:**2163–2170.
30. **Elliott G, Hafezi W, Whiteley A, Bernard E.** 2005. Deletion of the herpes simplex virus VP22-encoding gene (UL49) alters the expression, localization, and virion incorporation of ICP0. J. Virol. **79:**9735–9745. http://dx.doi.org/10.1128/JVI.79.15.9735-9745.2005.
31. **Bernstein BW, Bamburg JR.** 2010. ADF/cofilin: a functional node in cell biology. Trends Cell Biol. **20:**187–195. http://dx.doi.org/10.1016/j.tcb.2010.01.001.
32. **Wang Y, Shibasaki F, Mizuno K.** 2005. Calcium signal-induced cofilin dephosphorylation is mediated by slingshot via calcineurin. J. Biol. Chem. **280:**12683–12689.
33. **Mizuno K.** 2013. Signaling mechanisms and functional roles of cofilin phosphorylation and dephosphorylation. Cell. Signal. **25:**457–469. http://dx.doi.org/10.1016/j.cellsig.2012.11.001.
34. **Bierne H, Gouin E, Roux P, Caroni P, Yin HL, Cossart P.** 2001. A role for cofilin and LIM kinase in *Listeria*-induced phagocytosis. J. Cell Biol. **155:**101–121. http://dx.doi.org/10.1083/jcb.200104037.
35. **Chan AY, Bailly M, Zebda N, Segall JE, Condeelis JS.** 2000. Role of cofilin in epidermal growth factor-stimulated actin polymerization and lamellipod protrusion. J. Cell Biol. **148:**531–542. http://dx.doi.org/10.1083/jcb.148.3.531.
36. **Jovceva E, Larsen MR, Waterfield MD, Baum B, Timms JF.** 2007. Dynamic cofilin phosphorylation in the control of lamellipodial actin homeostasis. J. Cell Sci. **120:**1888–1897. http://dx.doi.org/10.1242/jcs.004366.

37. **Pei Y, Xiang YF, Chen JN, Lu CH, Hao J, Du Q, Lai CC, Qu C, Li S, Ju HQ, Ren Z, Liu QY, Xiong S, Qian CW, Zeng FL, Zhang PZ, Yang CR, Zhang YJ, Xu J, Kitazato K, Wang YF.** 2011. Pentagalloylglucose down-regulates cofilin1 and inhibits HSV-1 infection. Antiviral Res. **89:**98–108. http://dx.doi.org/10.1016/j.antiviral.2010.11.012.
38. **Hahn AS, Kaufmann JK, Wies E, Naschberger E, Panteleev-Ivlev J, Schmidt K, Holzer A, Schmidt M, Chen J, König S, Ensser A, Myoung J, Brockmeyer NH, Stürzl M, Fleckenstein B, Neipel F.** 2012. The ephrin receptor tyrosine kinase A2 is a cellular receptor for Kaposi's sarcoma–associated herpesvirus. Nat. Med. **18:**961–966. http://dx.doi.org/10.1038/nm.2805.
39. **Saeed MF, Kolokoltsov AA, Freiberg AN, Holbrook MR, Davey RA.** 2008. Phosphoinositide-3 kinase-Akt pathway controls cellular entry of Ebola virus. PLoS Pathog. **4:**e1000141. http://dx.doi.org/10.1371/journal.ppat.1000141.
40. **Izmailyan R, Hsao JC, Chung CS, Chen CH, Hsu PW, Liao CL, Chang W.** 2012. Integrin β1 mediates vaccinia virus entry through activation of PI3K/Akt signaling. J. Virol. **86:**6677–6687. http://dx.doi.org/10.1128/JVI.06860-11.
41. **Agerer F, Michel A, Ohlsen K, Hauck CR.** 2003. Integrin-mediated invasion of *Staphylococcus aureus* into human cells requires Src family protein-tyrosine kinases. J. Biol. Chem. **278:**42524–42531. http://dx.doi.org/10.1074/jbc.M302096200.
42. **Mainou BA, Dermody TS.** 2011. Src kinase mediates productive endocytic sorting of reovirus during cell entry. J. Virol. **85:**3203–3213. http://dx.doi.org/10.1128/JVI.02056-10.
43. **Wang X, Huong SM, Chiu ML, Raab-Traub N, Huang ES.** 2003. Epidermal growth factor receptor is a cellular receptor for human cytomegalovirus. Nature **424:**456–461. http://dx.doi.org/10.1038/nature01818.
44. **Chan G, Nogalski MT, Yurochko AD.** 2009. Activation of EGFR on monocytes is required for human cytomegalovirus entry and mediates cellular motility. Proc. Natl. Acad. Sci. U. S. A. **106:**22369–22374. http://dx.doi.org/10.1073/pnas.0908787106.
45. **Eierhoff T, Hrincius ER, Rescher U, Ludwig S, Ehrhardt C.** 2010. The epidermal growth factor receptor (EGFR) promotes uptake of influenza A viruses (IAV) into host cells. PLoS Pathog. **6:**e1001099. http://dx.doi.org/10.1371/journal.ppat.1001099.
46. **Lupberger J, Zeisel MB, Xiao F, Thumann C, Fofana I, Zona L, Davis C, Mee CJ, Turek M, Gorke S, Royer C, Fischer B, Zahid MN, Lavillette D, Fresquet J, Cosset FL, Rothenberg SM, Pietschmann T, Patel AH, Pessaux P, Doffoël M, Raffelsberger W, Poch O, Mckeating JA, Brino L, Baumert TF.** 2011. EGFR and EphA2 are host factors for hepatitis C virus entry and possible targets for antiviral therapy. Nat. Med. **17:**589–595. http://dx.doi.org/10.1038/nm.2341.
47. **Mineo C, James GL, Smart EJ, Anderson RG.** 1996. Localization of epidermal growth factor-stimulated Ras/Raf-1 interaction to caveolae membrane. J. Biol. Chem. **271:**11930–11935. http://dx.doi.org/10.1074/jbc.271.20.11930.
48. **Raghu H, Sharma-Walia N, Veettil MV, Sadagopan S, Caballero A, Sivakumar R, Varga L, Bottero V, Chandran B.** 2007. Lipid rafts of primary endothelial cells are essential for Kaposi's sarcoma-associated herpesvirus/human herpesvirus 8-induced phosphatidylinositol 3-kinase and RhoA-GTPases critical for microtubule dynamics and nuclear delivery of viral DNA but dispensable for binding and entry. J. Virol. **81:**7941–7959. http://dx.doi.org/10.1128/JVI.02848-06.
49. **Das S, Chakraborty S, Basu A.** 2010. Critical role of lipid rafts in virus entry and activation of phosphoinositide 3′ kinase/Akt signaling during early stages of Japanese encephalitis virus infection in neural stem/progenitor cells. J. Neurochem. **115:**537–549. http://dx.doi.org/10.1111/j.1471-4159.2010.06951.x.
50. **Meckes DG, Jr, Menaker NF, Raab-Traub N.** 2013. Epstein-Barr virus LMP1 modulates lipid raft microdomains and the vimentin cytoskeleton for signal transduction and transformation. J. Virol. **87:**1301–1311. http://dx.doi.org/10.1128/JVI.02519-12.
51. **Bender FC, Whitbeck JC, Ponce de Leon M, Lou H, Eisenberg RJ, Cohen GH.** 2003. Specific association of glycoprotein B with lipid rafts during herpes simplex virus entry. J. Virol. **77:**9542–9552. http://dx.doi.org/10.1128/JVI.77.17.9542-9552.2003.
52. **Pleschka S, Wolff T, Ehrhardt C, Hobom G, Planz O, Rapp UR, Ludwig S.** 2001. Influenza virus propagation is impaired by inhibition of the Raf/MEK/ERK signalling cascade. Nat. Cell Biol. **3:**301–305. http://dx.doi.org/10.1038/35060098.
53. **Naranatt PP, Akula SM, Zien CA, Krishnan HH, Chandran B.** 2003. Kaposi's sarcoma-associated herpesvirus induces the phosphatidylinositol 3-kinase-PKC-zeta-MEK-ERK signaling pathway in target cells early during infection: implications for infectivity. J. Virol. **77:**1524–1539. http://dx.doi.org/10.1128/JVI.77.2.1524-1539.2003.
54. **Wagner MJ, Smiley JR.** 2011. Herpes simplex virus requires VP11/12 to activate Src family kinase-phosphoinositide 3-kinase-Akt signaling. J. Virol. **85:**2803–2812. http://dx.doi.org/10.1128/JVI.01877-10.
55. **Romero S, Grompone G, Carayol N, Mounier J, Guadagnini S, Prevost MC, Sansonetti PJ, Van Nhieu GT.** 2011. ATP-mediated ERK1/2 activation stimulates bacterial capture by filopodia, which precedes *Shigella* invasion of epithelial cells. Cell Host Microbe **9:**508–519. http://dx.doi.org/10.1016/j.chom.2011.05.005.
56. **Mansfield PJ, Shayman JA, Boxer LA.** 2000. Regulation of polymorphonuclear leukocyte phagocytosis by myosin light chain kinase after activation of mitogen-activated protein kinase. Blood **95:**2407–2412.
57. **Pritchard CA, Hayes L, Wojnowski L, Zimmer A, Marais RM, Norman JC.** 2004. B-raf acts via the ROCKII/LIMK/Cofilin pathway to maintain actin stress fibers in fibroblasts. Mol. Cell. Biol. **24:**5937–5952. http://dx.doi.org/10.1128/MCB.24.13.5937-5952.2004.
58. **Klein RM, Spofford LS, Abel EV, Ortiz A, Aplin AE.** 2008. B-raf regulation of Rnd3 participates in actin cytoskeletal and focal adhesion organization. Mol. Biol. Cell **19:**498–508. http://dx.doi.org/10.1091/mbc.E07-09-0895.
59. **Frampton AR, Jr, Stolz DB, Uchida H, Goins WF, Cohen JB, Glorioso JC.** 2007. Equine herpesvirus 1 enters cells by two different pathways, and infection requires the activation of the cellular kinase ROCK1. J. Virol. **81:**10879–10889. http://dx.doi.org/10.1128/JVI.00504-07.
60. **Luo L.** 2000. Rho GTPases in neuronal morphogenesis. Nat. Rev. Neurosci. **1:**173–180. http://dx.doi.org/10.1038/35044547.
61. **Bamburg JR, Bernstein BW, Davis RC, Flynn KC, Goldsbury C, Jensen JR, Maloney MT, Minamide LS, Pak CW, Shaw AE, Whiteman I, Wiggan O.** 2010. ADF/cofilin-actin rods in neurodegenerative diseases. Curr. Alzheimer Res. **7:**241–250. http://dx.doi.org/10.2174/156720510791050902.
62. **Berkova Z, Crawford SE, Blutt SE, Morris AP, Estes MK.** 2007. Expression of rotavirus NSP4 alters the actin network organization through the actin remodeling protein cofilin. J. Virol. **81:**3545–3553. http://dx.doi.org/10.1128/JVI.01080-06.
63. **Stolp B, Reichman-Fried M, Abraham L, Pan X, Giese SI, Hannemann S, Goulimari P, Raz E, Grosse R, Fackler OT.** 2009. HIV-1 Nef interferes with host cell motility by deregulation of cofilin. Cell Host Microbe **6:**174–186. http://dx.doi.org/10.1016/j.chom.2009.06.004.
64. **Stolp B, Abraham L, Rudolph JM, Fackler OT.** 2010. Lentiviral Nef proteins utilize PAK2-mediated deregulation of cofilin as a general strategy to interfere with actin remodeling. J. Virol. **84:**3935–3948. http://dx.doi.org/10.1128/JVI.02467-09.
65. **Han X, Yu R, Ji L, Zhen D, Tao S, Li S, Sun Y, Huang L, Feng Z, Li X, Han G, Schmidt M, Han L.** 2011. InlB-mediated *Listeria monocytogenes* internalization requires a balanced phospholipase D activity maintained through phospho-cofilin. Mol. Microbiol. **81:**860–880. http://dx.doi.org/10.1111/j.1365-2958.2011.07726.x.
66. **Yoder A, Yu D, Dong L, Iyer SR, Xu X, Kelly J, Liu J, Wang W, Vorster PJ, Agulto L, Stephany DA, Cooper JN, Marsh JW, Wu Y.** 2008. HIV envelope-CXCR4 signaling activates cofilin to overcome cortical actin restriction in resting CD4 T cells. Cell **134:**782–792. http://dx.doi.org/10.1016/j.cell.2008.06.036.
67. **Cameron PU, Saleh S, Sallmann G, Solomon A, Wightman F, Evans VA, Boucher G, Haddad EK, Sekaly RP, Harman AN, Anderson JL, Jones KL, Mak J, Cunningham AL, Jaworowski A, Lewin SR.** 2010. Establishment of HIV-1 latency in resting CD4+ T cells depends on chemokine-induced changes in the actin cytoskeleton. Proc. Natl. Acad. Sci. U. S. A. **107:**16934–16939. http://dx.doi.org/10.1073/pnas.1002894107.
68. **Sharma-Walia N, Krishnan HH, Naranatt PP, Zeng L, Smith MS, Chandran B.** 2005. ERK1/2 and MEK1/2 induced by Kaposi's sarcoma-associated herpesvirus (human herpesvirus 8) early during infection of target cells are essential for expression of viral genes and for establishment of infection. J. Virol. **79:**10308–10329. http://dx.doi.org/10.1128/JVI.79.16.10308-10329.2005.
69. **Tiwari V, Shukla D.** 2010. Phosphoinositide 3 kinase signalling may affect multiple steps during herpes simplex virus type-1 entry. J. Gen. Virol. **91:**3002–3009. http://dx.doi.org/10.1099/vir.0.024166-0.

70. **Chuluunbaatar U, Roller R, Mohr I.** 2012. Suppression of extracellular signal-regualated kinase activity in herpes simplex virus 1-infected cells by the Us3 protein kinase. J. Virol. **86:**7771–7776. http://dx.doi.org/10.1128/JVI.00622-12.
71. **Torres NI, Castilla V, Bruttomesso AC, Eiras J, Galagovsky LR, Wachsman MB.** 2012. In vitro antiviral activity of dehydroepiandrosterone, 17 synthetic analogs and ERK modulators against herpes simplex virus type 1. Antiviral Res. **95:**37–48. http://dx.doi.org/10.1016/j.antiviral.2012.05.002.
72. **Antoine TE, Shukla D. 28** June 2013. Inhibition of myosin light chain kinase can be targeted for the development of new therapies against HSV-1 infection. Antivir. Ther. http://dx.doi.org/10.3851/IMP2661.
73. **Valiya Veettil M, Sadagopan S, Kerur N, Chakraborty S, Chandran B.** 2010. Interaction of c-Cbl with myosin IIA regulates bleb associated macropinocytosis of Kaposi's sarcoma-associated herpesvirus. PLoS Pathog. **6:**e1001238. http://dx.doi.org/10.1371/journal.ppat.1001238.
74. **Greene W, Gao SJ.** 2009. Actin dynamics regulates multiple endosomal steps during Kaposi's sarcoma-associated herpesvirus entry and trafficking in endothelial cells. PLoS Pathog. **5:**e1000512. http://dx.doi.org/10.1371/journal.ppat.1000512.